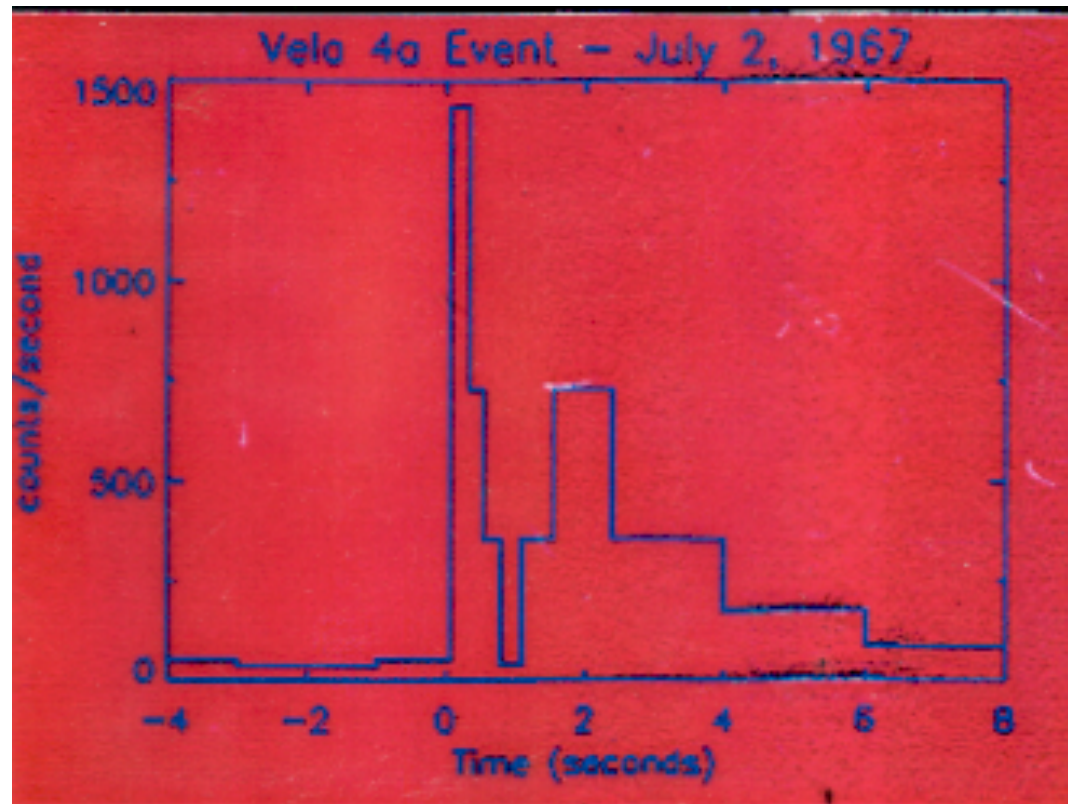


# Lecture 20

## *Gamma-Ray Bursts*

## *First Gamma-Ray Burst*

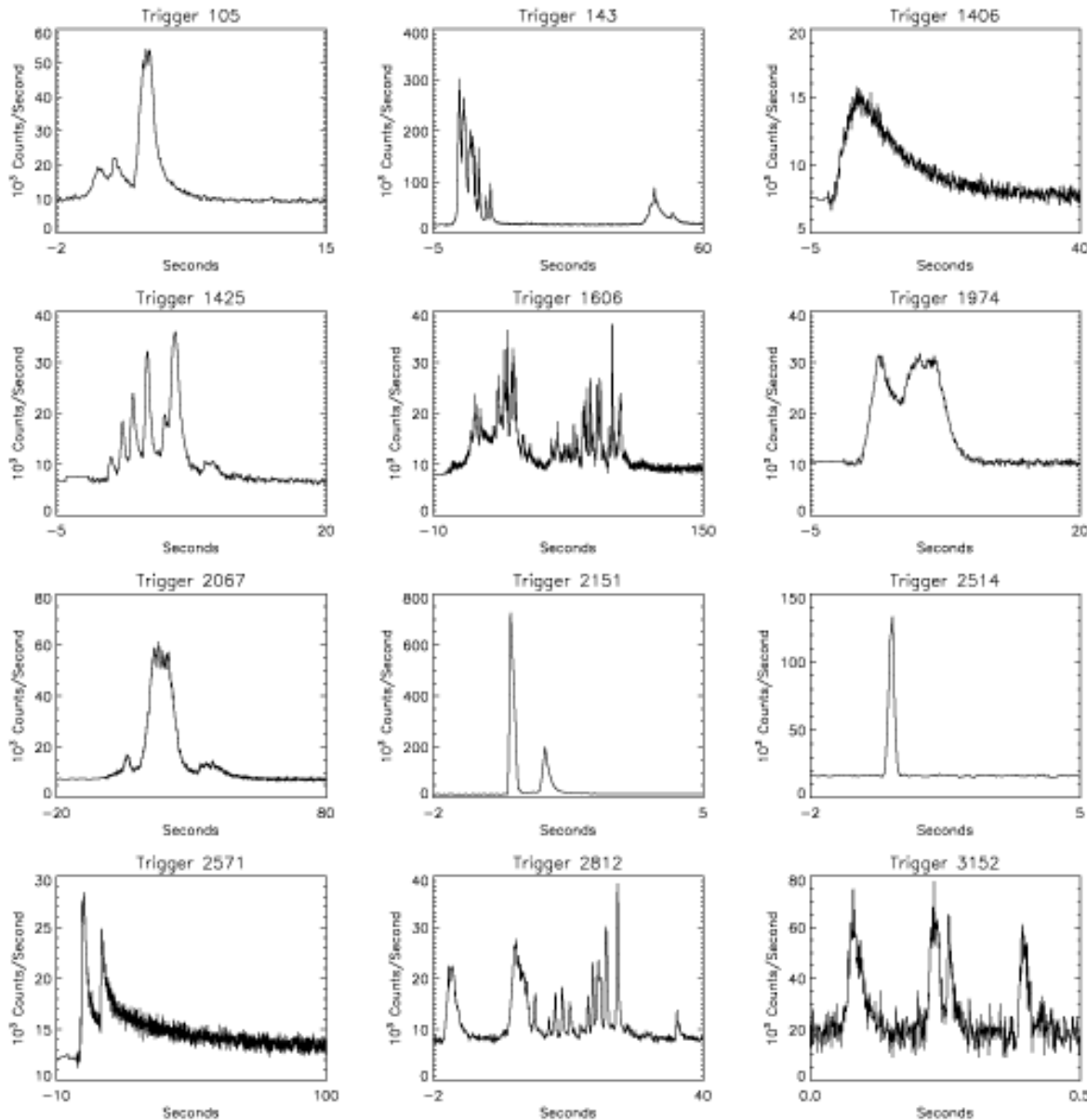


*The Vela 5 satellites functioned from July, 1969 to April, 1979 and detected a total of 73 gamma-ray bursts in the energy range 150 – 750 keV (n.b., Greater than 30 keV is gamma-rays). Discovery reported Klebesadel, Strong, and Olson (1973).*



Ian Strong – left Ray Klebesadel – right  
September 16, 2003

Gamma-ray bursts (GRBs) discovered 1969 - 72 by Vela  
satellites. Published by Klebesadel, Strong and Olson (1973)

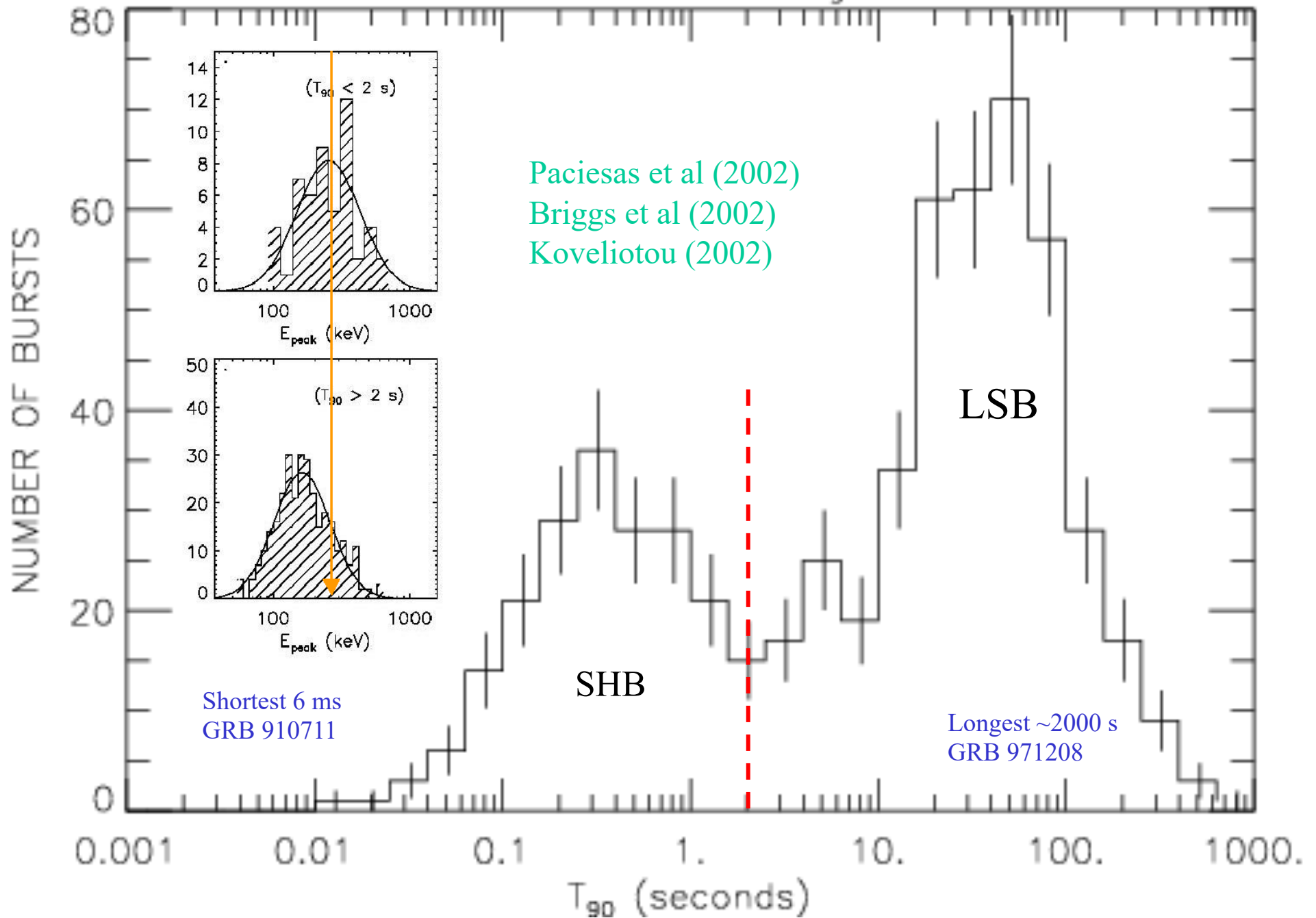


Typical durations are 20 seconds but there is wide variation both in time-structure and duration.

Some last only hundredths of a second. Others last thousands of seconds. The longest so far is 10,000 s

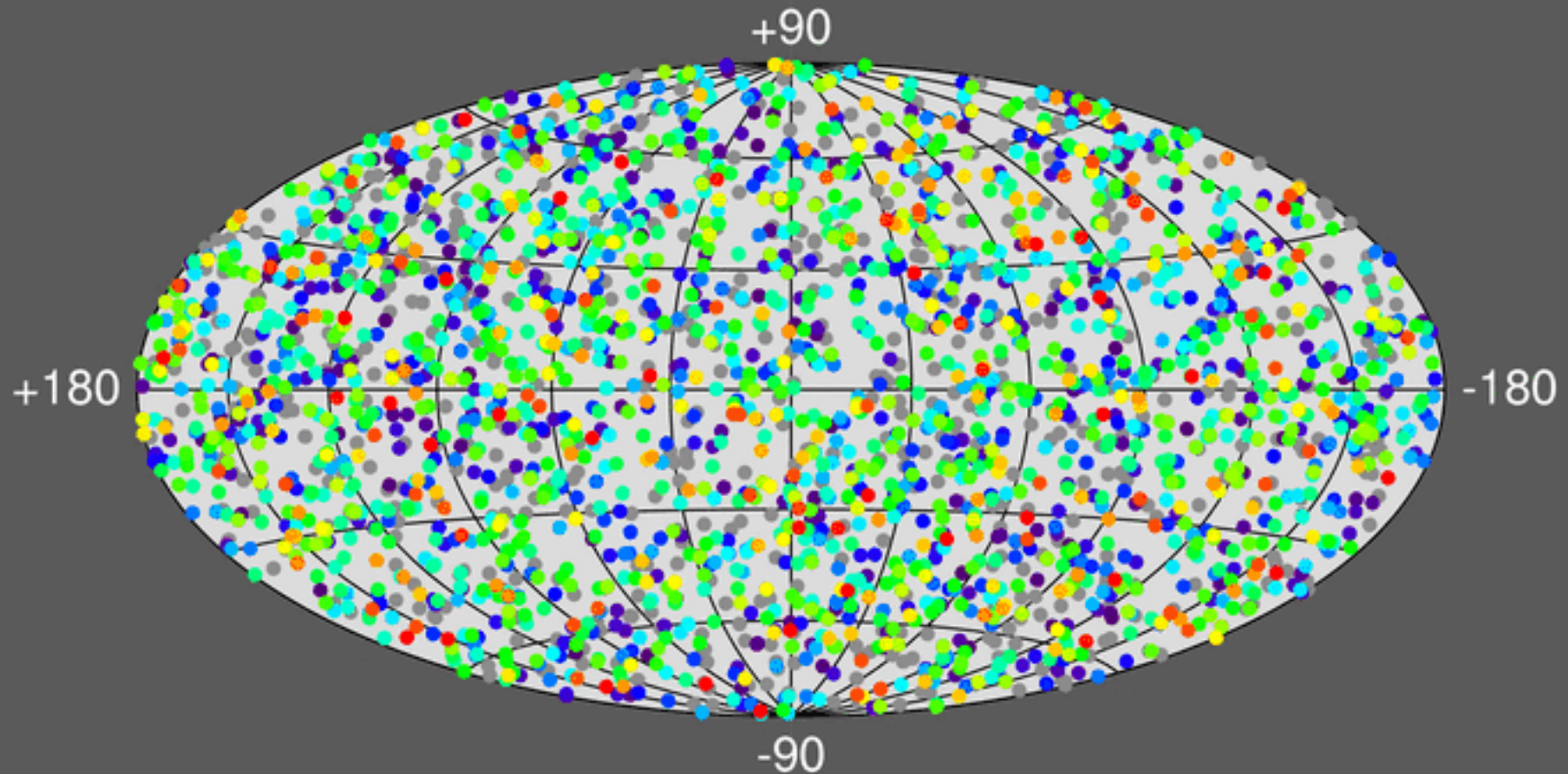
Typical power spectra peak at 200 keV and higher.

# BATSE 4B Catalog



April 27, 2013 with Fermi and Swift lasted almost a day in GeV radiation

# 2704 BATSE Gamma-Ray Bursts



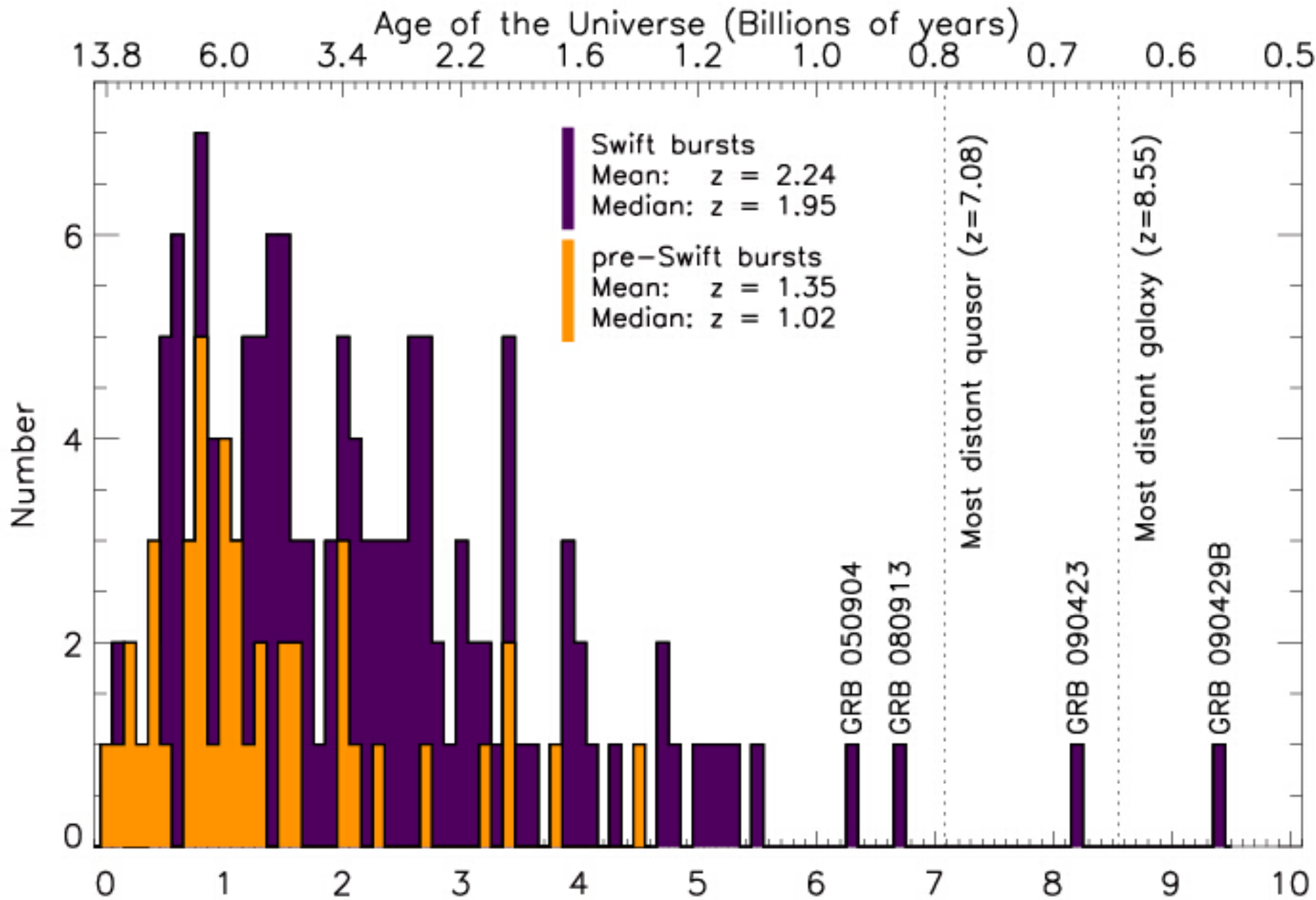
In total about 5000 gamma-ray bursts had been detected by 2004  
SWIFT spotted an additional 1000 GRBs by 2015.

*Skipping over a rich  
history here*

Table 1

#	Author	Year Pub	Reference	Main Body	2nd Body	Place	Description
1.	Colgate	1968	CJPhys, 46, S476	ST		COS	SN shocks stellar surface in distant galaxy
2.	Colgate	1974	ApJ, 187, 333	ST		COS	Type II SN shock brem, inv Comp scat at stellar surface
3.	Stecker et al.	1973	Nature, 245, PS70	ST		DISK	Stellar superflare from nearby star
4.	Stecker et al.	1973	Nature, 245, PS70	WD		DISK	Superflare from nearby WD
5.	Harwit et al.	1973	ApJ, 186, L37	NS	COM	DISK	Relic comet perturbed to collide with old galactic NS
6.	Lamb et al.	1973	Nature, 246, PS52	WD	ST	DISK	Accretion onto WD from flare in companion
7.	Lamb et al.	1973	Nature, 246, PS52	NS	ST	DISK	Accretion onto NS from flare in companion
8.	Lamb et al.	1973	Nature, 246, PS52	BH	ST	DISK	Accretion onto BH from flare in companion
9.	Zwicky	1974	Ap & SS, 28, 111	NS		HALO	NS chunk contained by external pressure escapes, explodes
10.	Grindlay et al.	1974	ApJ, 187, L93	DG		SOL	Relativistic iron dust grain up-scatters solar radiation
11.	Brecher et al.	1974	ApJ, 187, L97	ST		DISK	Directed stellar flare on nearby star
12.	Schlovskii	1974	SovAstron, 18, 390	WD	COM	DISK	Comet from system's cloud strikes WD
13.	Schlovskii	1974	SovAstron, 18, 390	NS	COM	DISK	Comet from system's cloud strikes NS
14.	Bisnovatyi- et al.	1975	Ap & SS, 35, 23	ST		COS	Absorption of neutrino emission from SN in stellar envelope
15.	Bisnovatyi- et al.	1975	Ap & SS, 35, 23	ST	SN	COS	Thermal emission when small star heated by SN shock wave
16.	Bisnovatyi- et al.	1975	Ap & SS, 35, 23	NS		COS	Ejected matter from NS explodes
17.	Pacini et al.	1974	Nature, 251, 399	NS		DISK	NS crustal starquake glitch; should time coincide with GRB
18.	Narlikar et al.	1974	Nature, 251, 590	WH		COS	White hole emits spectrum that softens with time
19.	Tsygan	1975	A&A, 44, 21	NS		HALO	NS corequake excites vibrations, changing E & B fields
20.	Chanmugam	1974	ApJ, 193, L75	WD		DISK	Convection inside WD with high B field produces flare
21.	Prilutski et al.	1975	Ap & SS, 34, 395	AGN	ST	COS	Collapse of supermassive body in nucleus of active galaxy
22.	Narlikar et al.	1975	Ap & SS, 35, 321	WH		COS	WH excites synchrotron emission, inverse Compton scattering
23.	Piran et al.	1975	Nature, 256, 112	BH		DISK	Inv Comp scat deep in ergosphere of fast rotating, accreting BH
24.	Fabian et al.	1976	Ap & SS, 42, 77	NS		DISK	NS crustquake shocks NS surface
25.	Chanmugam	1976	Ap & SS, 42, 83	WD		DISK	Magnetic WD suffers MHD instabilities, flares
26.	Mullan	1976	ApJ, 208, 199	WD		DISK	Thermal radiation from flare near magnetic WD
27.	Woosley et al.	1976	Nature, 263, 101	NS		DISK	Carbon detonation from accreted matter onto NS
28.	Lamb et al.	1977	ApJ, 217, 197	NS		DISK	Mag grating of accret disk around NS causes sudden accretion
29.	Piran et al.	1977	ApJ, 214, 268	BH		DISK	Instability in accretion onto rapidly rotating BH
30.	Dasgupta	1979	Ap & SS, 63, 517	DG		SOL	Charged intergal rel dust grain enters sol sys, breaks up
31.	Tsygan	1980	A&A, 87, 224	WD		DISK	WD surface nuclear burst causes chromospheric flares
32.	Tsygan	1980	A&A, 87, 224	NS		DISK	NS surface nuclear burst causes chromospheric flares
33.	Ramaty et al.	1981	Ap & SS, 75, 193	NS		DISK	NS vibrations heat atm to pair produce, annihilate, synch cool
34.	Newman et al.	1980	ApJ, 242, 319	NS	AST	DISK	Asteroid from interstellar medium hits NS
35.	Ramaty et al.	1980	Nature, 287, 122	NS		HALO	NS core quake caused by phase transition, vibrations
36.	Howard et al.	1981	ApJ, 249, 302	NS	AST	DISK	Asteroid hits NS, B-field confines mass, creates high temp
37.	Mitrofanov et al.	1981	Ap & SS, 77, 469	NS		DISK	Helium flash cooled by MHD waves in NS outer layers
38.	Colgate et al.	1981	ApJ, 248, 771	NS	AST	DISK	Asteroid hits NS, tidally disrupts, heated, expelled along B lines
39.	van Buren	1981	ApJ, 249, 297	NS	AST	DISK	Asteroid enters NS B field, dragged to surface collision
40.	Kuznetsov	1982	CosRes, 20, 72	MG		SOL	Magnetic reconnection at heliopause
41.	Katz	1982	ApJ, 260, 371	NS		DISK	NS flares from pair plasma confined in NS magnetosphere
42.	Woosley et al.	1982	ApJ, 258, 716	NS		DISK	Magnetic reconnection after NS surface He flash
43.	Fryxell et al.	1982	ApJ, 258, 733	NS		DISK	He fusion runaway on NS B-pole helium lake
44.	Hameury et al.	1982	A&A, 111, 242	NS		DISK	e- capture triggers H flash triggers He flash on NS surface
45.	Mitrofanov et al.	1982	MNRAS, 200, 1033	NS		DISK	B induced cyclo res in rad absorp giving rel e-s, inv C scat
46.	Fenimore et al.	1982	Nature, 297, 665	NS		DISK	BB X-rays inv Comp scat by hotter overlying plasma
47.	Lipunov et al.	1982	Ap & SS, 85, 459	NS	ISM	DISK	ISM matter accum at NS magnetopause then suddenly accretes
48.	Baan	1982	ApJ, 261, L71	WD		HALO	Nonexplosive collapse of WD into rotating, cooling NS
49.	Ventura et al.	1983	Nature, 301, 491	NS	ST	DISK	NS accretion from low mass binary companion
50.	Bisnovatyi- et al.	1983	Ap & SS, 89, 447	NS		DISK	Neutron rich elements to NS surface with quake, undergo fission
51.	Bisnovatyi- et al.	1984	SovAstron, 28, 62	NS		DISK	Thermonuclear explosion beneath NS surface
52.	Ellison et al.	1983	A&A, 128, 102	NS		HALO	NS corequake + uneven heating yield SGR pulsations
53.	Hameury et al.	1983	A&A, 128, 369	NS		DISK	B field contains matter on NS cap allowing fusion
54.	Bonazzola et al.	1984	A&A, 136, 89	NS		DISK	NS surface nuc explosion causes small scale B reconnection
55.	Michel	1985	ApJ, 290, 721	NS		DISK	Remnant disk ionization instability causes sudden accretion
56.	Liang	1984	ApJ, 283, L21	NS		DISK	Resonant EM absorp during magnetic flare gives hot sync e-s
57.	Liang et al.	1984	Nature, 310, 121	NS		DISK	NS magnetic fields get twisted, recombine, create flare
58.	Mitrofanov	1984	Ap & SS, 105, 245	NS		DISK	NS magnetosphere excited by starquake
59.	Epstein	1985	ApJ, 291, 822	NS		DISK	Accretion instability between NS and disk
60.	Schlovskii et al.	1985	MNRAS, 212, 545	NS		HALO	Old NS in Galactic halo undergoes starquake
61.	Tsygan	1984	Ap & SS, 106, 199	NS		DISK	Weak B field NS spherically accretes, Comptonizes X-rays
62.	Usov	1984	Ap & SS, 107, 191	NS		DISK	NS flares result of magnetic convective-oscillation instability
63.	Hameury et al.	1985	ApJ, 293, 56	NS		DISK	High Landau e-s beamed along B lines in cold atm of NS
64.	Rappaport et al.	1985	Nature, 314, 242	NS		DISK	NS + low mass stellar companion gives GRB + optical flash
65.	Tremaine et al.	1986	ApJ, 301, 155	NS	COM	DISK	NS tides disrupt comet, debris hits NS next pass
66.	Muslimov et al.	1986	Ap & SS, 120, 27	NS		HALO	Radially oscillating NS
67.	Sturrock	1986	Nature, 321, 47	NS		DISK	Flare in the magnetosphere of NS accelerates e-s along B-field
68.	Paczynski	1986	ApJ, 308, L43	NS		COS	Cosmo GRBs: rel e- e+ opt thk plasma outflow indicated
69.	Bisnovatyi- et al.	1986	SovAstron, 30, 582	NS		DISK	Chain fission of superheavy nuclei below NS surface during SN
70.	Alcock et al.	1986	PLR, 57, 2088	SS	SS	DISK	SN ejects strange mat lump craters rotating SS companion
71.	Vahia et al.	1988	A&A, 207, 55	ST		DISK	Magnetically active stellar system gives stellar flare
72.	Babul et al.	1987	ApJ, 316, L49	CS		COS	GRB result of energy released from cusp of cosmic string
73.	Livio et al.	1987	Nature, 327, 398	NS	COM	DISK	Oort cloud around NS can explain soft gamma-repeaters
74.	McBreen et al.	1988	Nature, 332, 234	GAL	AGN	COS	G-wave bkgrd makes BL Lac wiggle across galaxy lens caustic

75.	Curtis	1988	ApJ, 327, L81	WD		COS	WD collapses, burns to form new class of stable particles
76.	Melia	1988	ApJ, 335, 965	NS		DISK	Be/X-ray binary sys evolves to NS accretion GRB with recurrence
77.	Ruderman et al.	1988	ApJ, 335, 306	NS		DISK	e+ e- cascades by aligned pulsar outer-mag-sphere reignition
78.	Paczynski	1988	ApJ, 335, 525	CS		COS	Energy released from cusp of cosmic string (revised)
79.	Murikami et al.	1988	Nature, 335, 234	NS		DISK	Absorption features suggest separate colder region near NS
80.	Melia	1988	Nature, 336, 658	NS		DISK	NS + accretion disk reflection explains GRB spectra
81.	Blaes et al.	1989	ApJ, 343, 839	NS		DISK	NS seismic waves couple to magnetospheric Alfen waves
82.	Trofimenko et al.	1989	Ap & SS, 152, 105	WH		COS	Kerr-Newman white holes
83.	Sturrock et al.	1989	ApJ, 346, 950	NS		DISK	NS E-field accelerates electrons which then pair cascade
84.	Fenimore et al.	1988	ApJ, 335, L71	NS		DISK	Narrow absorption features indicate small cold area on NS
85.	Rodrigues	1989	AJ, 98, 2280	WD	WD	DISK	Binary member loses part of crust, through L1, hits primary
86.	Pineault et al.	1989	ApJ, 347, 1141	NS	COM	DISK	Fast NS wanders through Oort clouds, fast WD bursts only optical
87.	Melia et al.	1989	ApJ, 346, 378	NS		DISK	Episodic electrostatic accel and Comp scat from rot high-B NS
88.	Trofimenko	1989	Ap & SS, 159, 301	WH		COS	Different types of white, "grey" holes can emit GRBs
* 89.	Eichler et al.	1989	Nature, 340, 126	NS	NS	COS	NS - NS binary members collide, coalesce
90.	Wang et al.	1989	PRL, 63, 1550	NS		DISK	Cyclo res & Raman scat fits 20, 40 keV dips, magnetized NS
91.	Alexander et al.	1989	ApJ, 344, L1	NS		DISK	QED mag resonant opacity in NS atmosphere
92.	Melia	1990	ApJ, 351, 601	NS		DISK	NS magnetospheric plasma oscillations
93.	Ho et al.	1990	ApJ, 348, L25	NS		DISK	Beaming of radiation necessary from magnetized neutron stars
94.	Mitrofanov et al.	1990	Ap & SS, 165, 137	NS	COM	DISK	Interstellar comets pass through dead pulsar's magnetosphere
95.	Dermer	1990	ApJ, 360, 197	NS		DISK	Compton scattering in strong NS magnetic field
96.	Blaes et al.	1990	ApJ, 363, 612	NS	ISM	DISK	Old NS accretes from ISM, surface goes nuclear
97.	Paczynski	1990	ApJ, 363, 218	NS	NS	COS	NS-NS collision causes neutrino collisions, drives super-Ed wind
98.	Zdziarski et al.	1991	ApJ, 366, 343	RE	MBR	COS	Scattering of microwave background photons by rel e-s
99.	Pineault	1990	Nature, 345, 233	NS	COM	DISK	Young NS drifts through its own Oort cloud
100.	Trofimenko et al.	1991	Ap & SS, 178, 217	WH		HALO	White hole supernova gave simultaneous burst of g-waves from 1987A
101.	Melia et al.	1991	ApJ, 373, 198	NS		DISK	NS B-field undergoes resistive tearing, accelerates plasma
102.	Holcomb et al.	1991	ApJ, 378, 682	NS		DISK	Alfen waves in non-uniform NS atmosphere accelerate particles
103.	Haensel et al.	1991	ApJ, 375, 209	SS	SS	COS	Strange stars emit binding energy in grav rad and collide
104.	Blaes et al.	1991	ApJ, 381, 210	NS	ISM	DISK	Slow interstellar accretion onto NS, e- capture starquakes result
105.	Frank et al.	1992	ApJ, 385, L45	NS		DISK	Low mass X-ray binary evolve into GRB sites
106.	Woosley et al.	1992	ApJ, 391, 228	NS		HALO	Accreting WD collapsed to NS
107.	Dar et al.	1992	ApJ, 388, 164	WD		COS	WD accretes to form naked NS, GRB, cosmic rays
108.	Hanami	1992	ApJ, 389, L71	NS	PLAN	COS	NS - planet magnetospheric interaction unstable
109.	Meszaros et al.	1992	ApJ, 397, 570	NS	NS	COS	NS - NS collision produces anisotropic fireball
110.	Carter	1992	ApJ, 391, L67	BH	ST	COS	Normal stars tidally disrupted by galactic nucleus BH
111.	Usov	1992	Nature, 357, 472	NS		COS	WD collapses to form NS, B-field brakes NS rotation instantly
112.	Narayan et al.	1992	ApJ, 395, L83	NS	NS	COS	NS - NS merger gives optically thick fireball
113.	Narayan et al.	1992	ApJ, 395, L83	BH	NS	COS	BH - NS merger gives optically thick fireball
114.	Brainerd	1992	ApJ, 394, L33	AGN	JET	COS	Synchrotron emission from AGN jets
115.	Meszaros et al.	1992	MNRAS, 257, 29P	BH	NS	COS	BH-NS have neutrinos collide to gammas in clean fireball
116.	Meszaros et al.	1992	MNRAS, 257, 29P	NS	NS	COS	NS-NS have neutrinos collide to gammas in clean fireball
117.	Cline et al.	1992	ApJ, 401, L57	BH		DISK	Primordial BHs evaporating could account for short hard GRBs
118.	Rees et al.	1992	MNRAS, 258, 41P	NS	ISM	COS	Relativistic fireball reconverted to radiation when hits ISM



Now there is a galaxy<sup>z</sup> at  $z = 11.1$  GN-z11 discovered in 2016  
400 My after the Big Bang

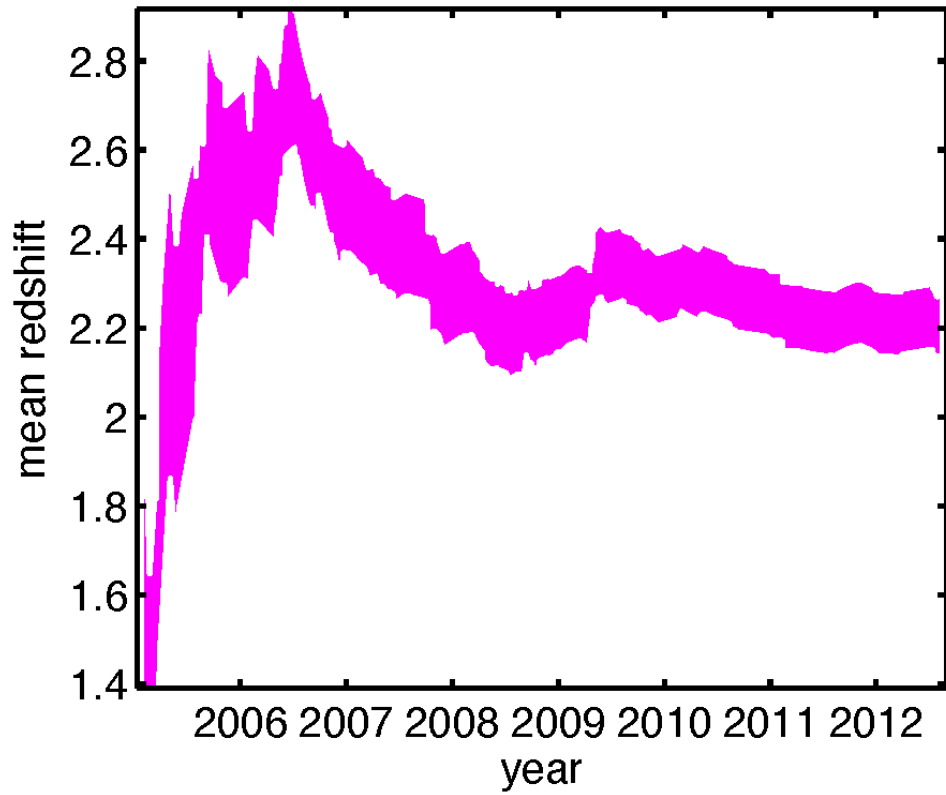


**Figure 1.** The *Swift* mean redshift uncertainty bound plotted over the duration of the mission. It is clear there is a drift in the mean redshift over time, a consequence of different priorities and instruments contributing to redshift acquisition i.e. the learning curve effect (see Coward 2009). The *jump* observed in 2009 is a result of GRBs 090423 and 090429B, with redshifts of  $z = 8.26$  (NIR spectroscopic) and  $z = 9.2$  (photometric) respectively.

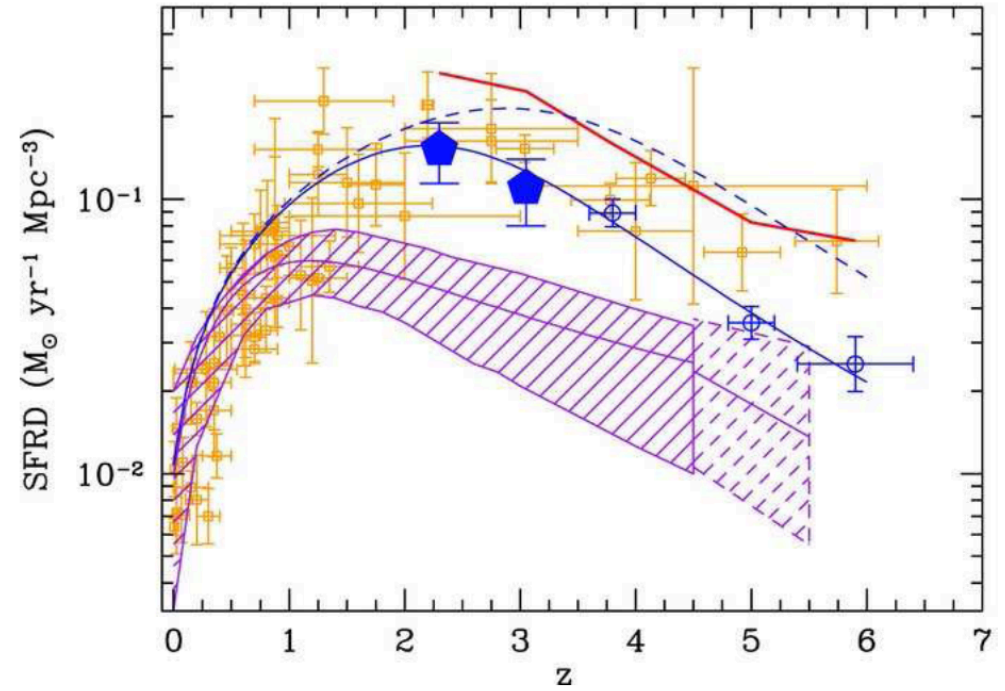
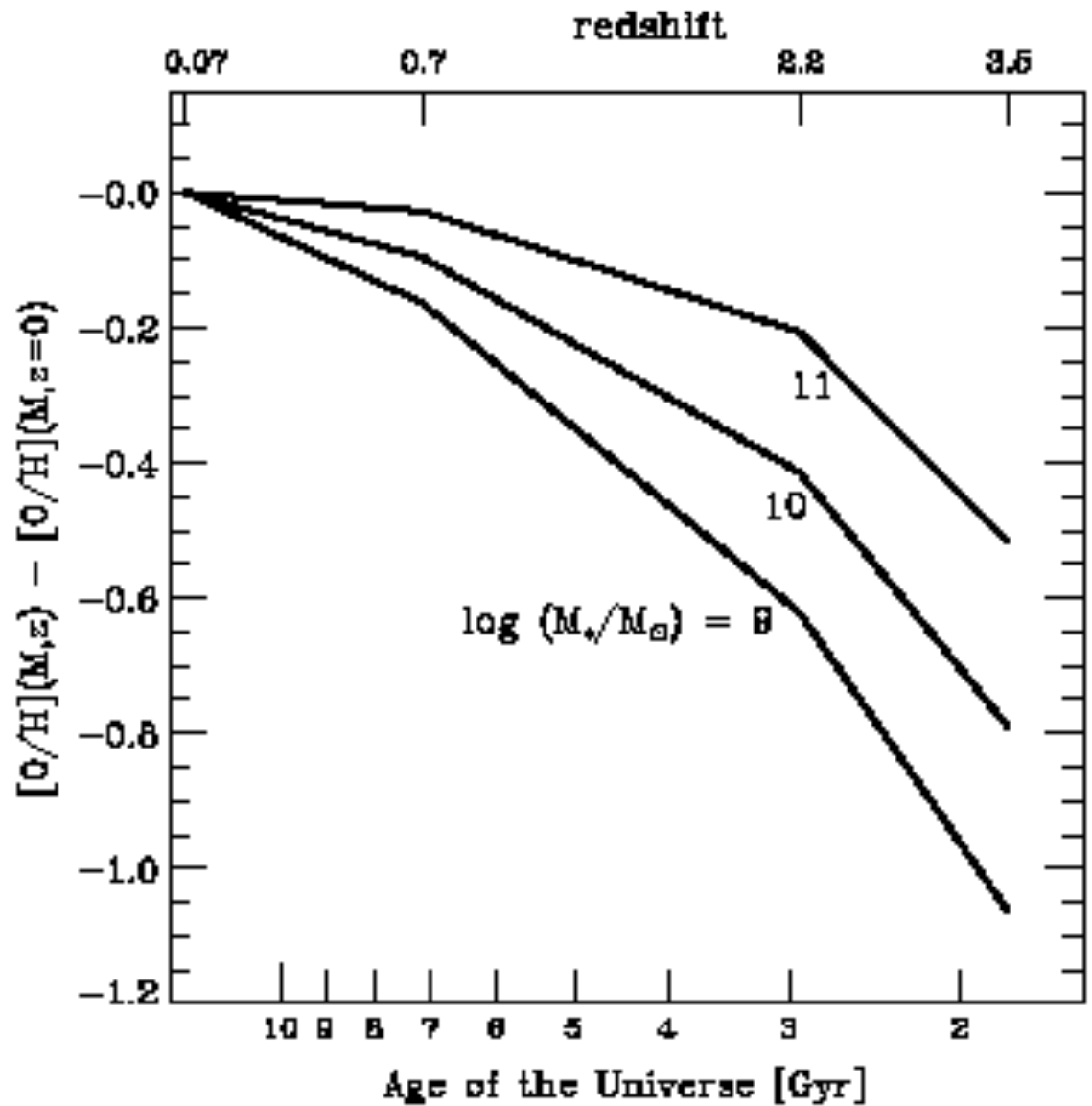


**Figure 5. Top panel:** Star formation rate history from multi-wavelength surveys taken from Fig. 10 in Reddy & Steidel (2009) and reproduced by permission of the AAS. We use the solid line, for the best-fit star-formation history assuming a luminosity-dependent dust correction to  $z \approx 2$ . See Appendix B for the conversion between the SFR and GRB rate evolution model,  $e(z)$ .



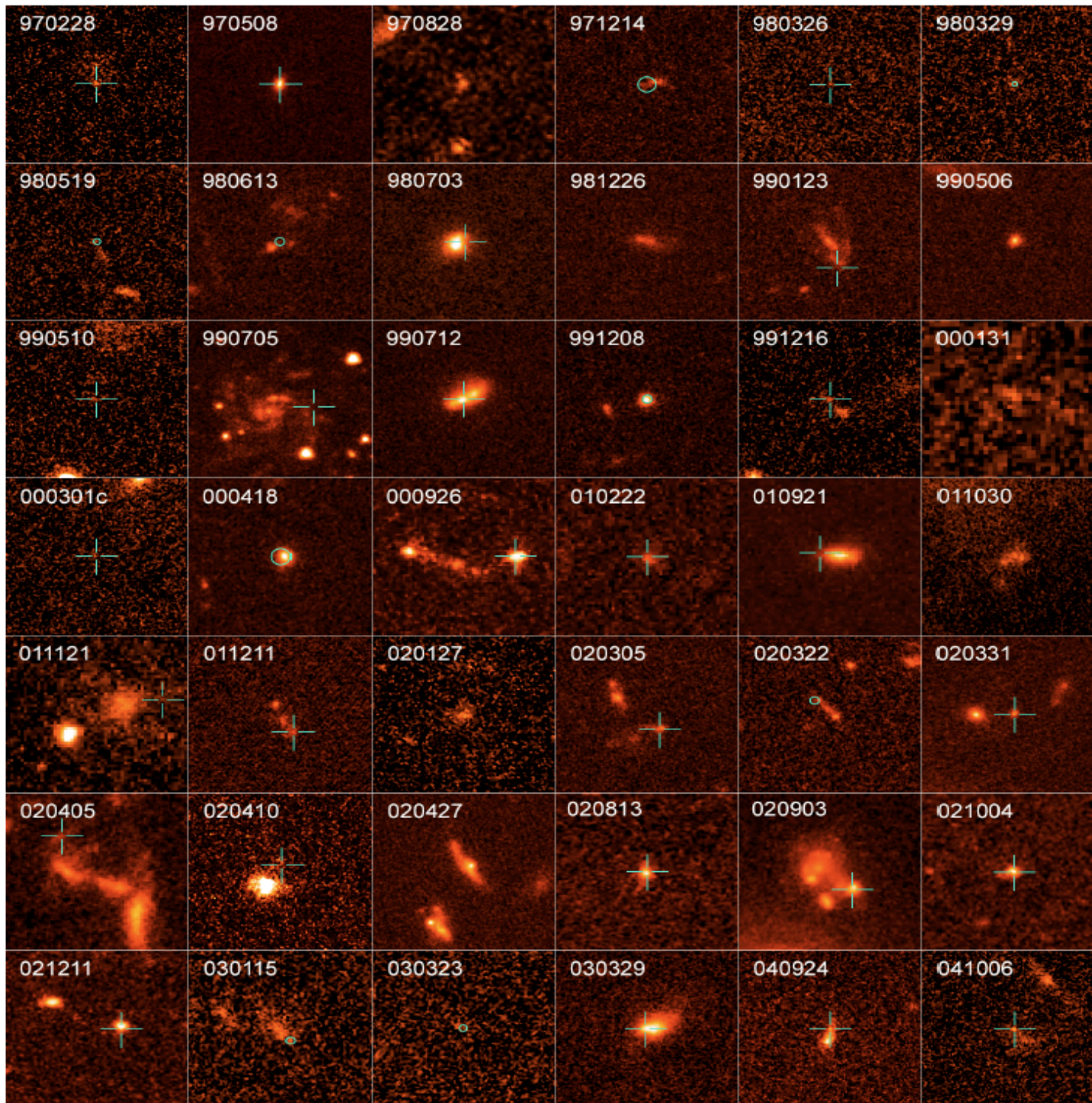
Maiolino et al (2008)

AMAZE Survey  
ESO-VLT

$Z \sim 2 - 3$  is an era of intense evolution for the SN rate and the metallicity

Metallicity in low M galaxies rises slower than in high M

nb. Z here is oxygen, not Fe; Fe/O declines with decreasing Z

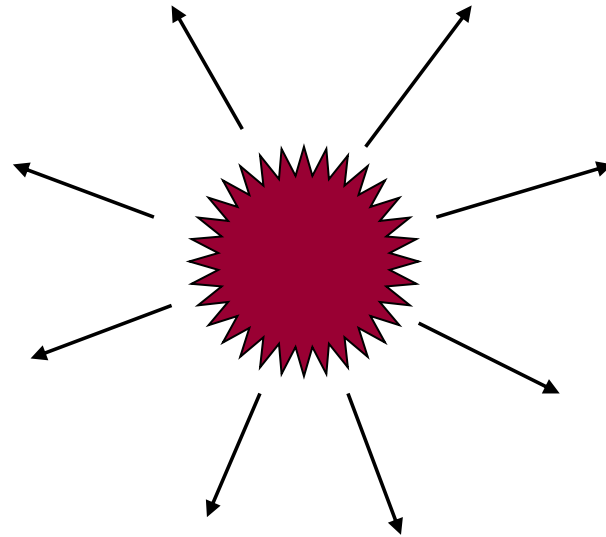


Fruchter et al. (2006)

*LSGRBs are found in star-forming galaxies. Their location within those galaxies is associated with the light with a tighter correlation than even Type Iip supernovae (but maybe not Type Ic).*

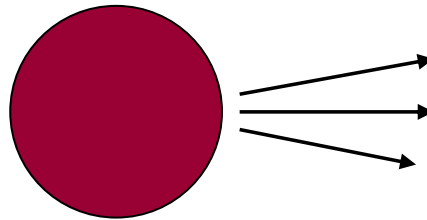
*At these distances gamma-ray bursts would have an energy of  $10^{52}$  erg to  $10^{54}$  erg if they emitted isotropically. That is up to the rest mass of the sun turned into gamma-rays in 10 seconds!*

But the energies required are not really that great



●  
*Earth*

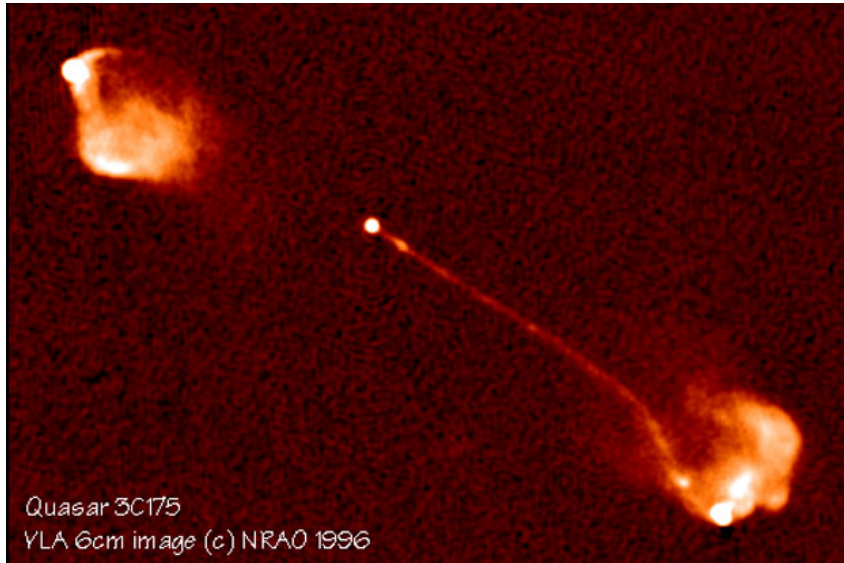
*If the energy were  
beamed to 0.1% of the  
sky, then the total  
energy could be  
1000 times less*



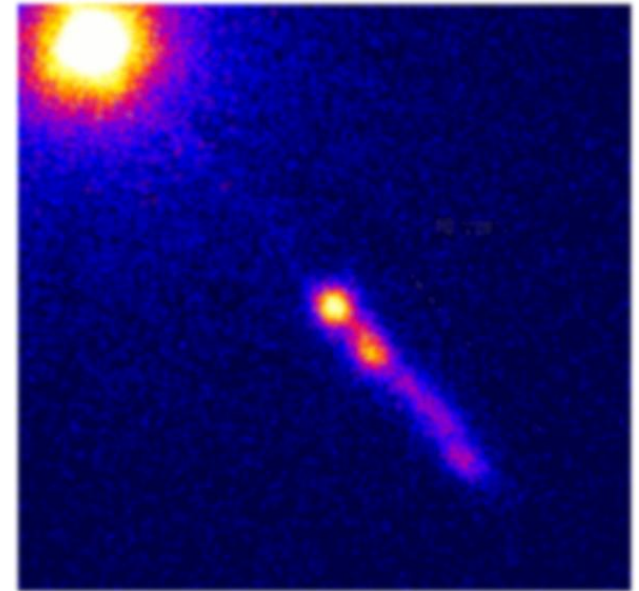
●  
*Earth*

*Nothing seen down here*

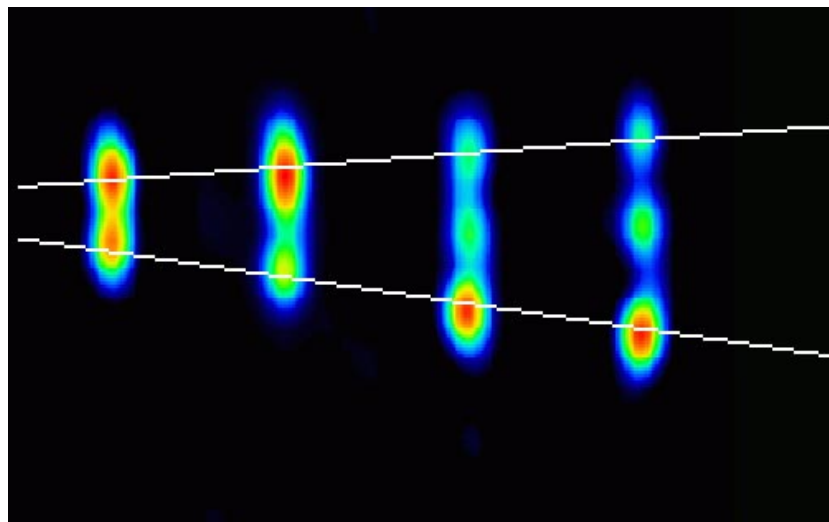
- GRBs are produced by highly relativistic flows that have been collimated into narrowly focused jets



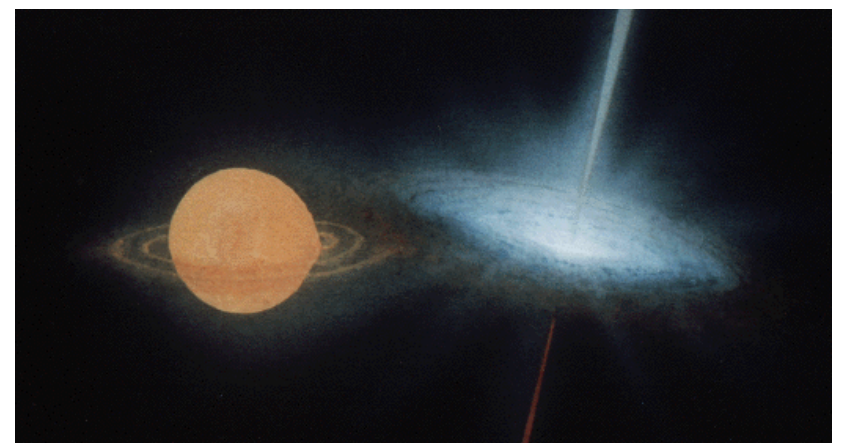
Quasar 3C 175 as seen in the radio



Quasar 3C273 as seen by the Chandra x-ray Observatory



Microquasar GPS 1915  
in our own Galaxy – time sequence



Artist's conception of SS433  
based on observations

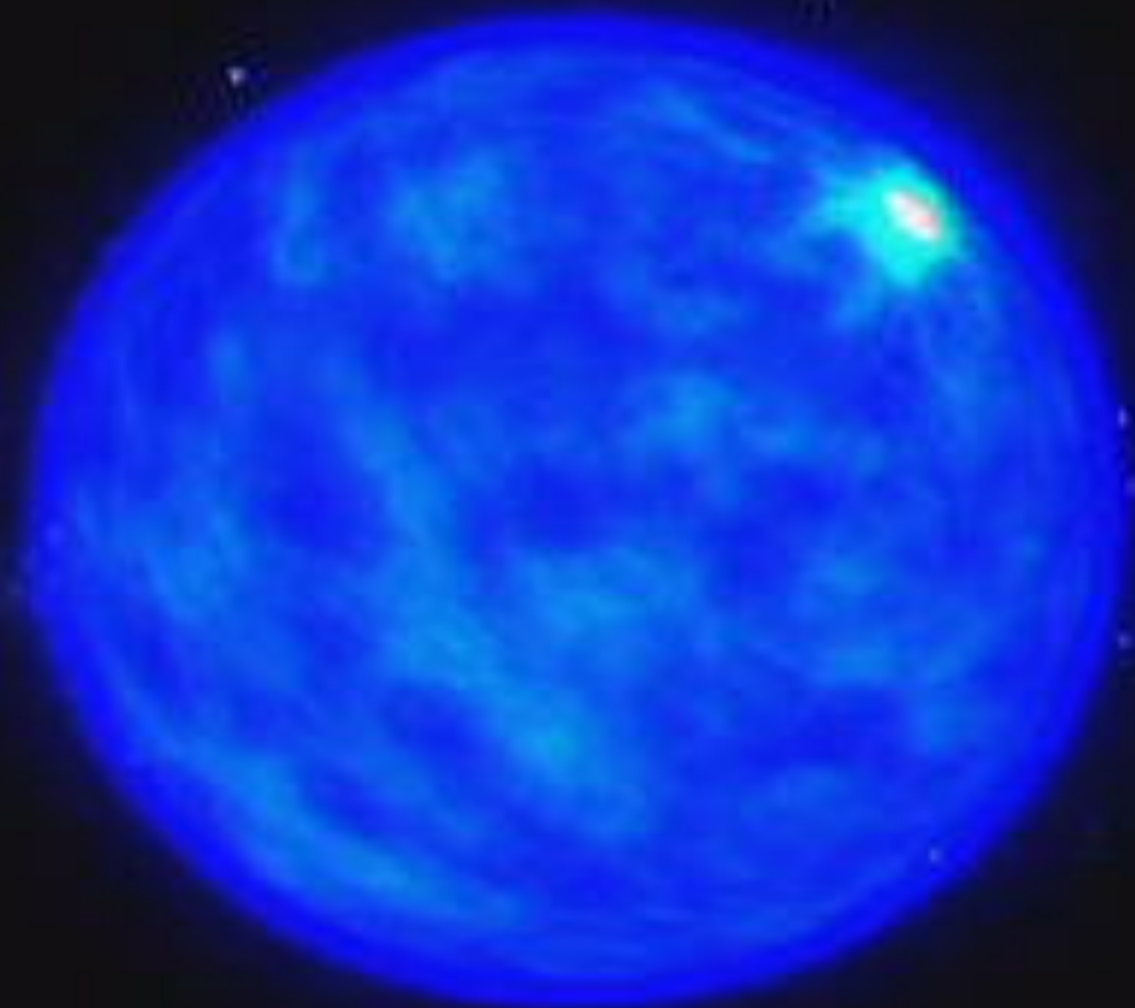


**Table 3**

CITED IN TEXT | ASCII | TYPESET IMAGE | 

Limits on Selected Bursts

GRB	$f_1$	$\alpha$	$e_{\text{max}}/m_e c^2$	$z$	$\hat{\tau}$	Limit A	Limit B	Reference
Bursts with Very High Energy Photons								
910503...	8.71	2.2	333	1	$3.0 \times 10^{12}$	<b>340</b>	300	1
910601...	0.5	2.8	9.8	1	$1.8 \times 10^{11}$	72	<b>110</b>	2
910814...	13.5	2.8	117	1	$4.7 \times 10^{12}$	<b>200</b>	190	3
930131...	1.95	2.0	1957	1	$7.0 \times 10^{11}$	<b>420</b>	270	4
940217...	0.36	2.5	6614	1	$1.2 \times 10^{11}$	<b>340</b>	120	5
950425...	1.62	1.93	235	1	$6.0 \times 10^{11}$	<b>300</b>	280	6
990123...	1.1	2.71	37	1.6	$1.2 \times 10^{12}$	150	<b>180</b>	7
Bursts with Redshifts								
971214...	0.35	2	1	3.42	$2.6 \times 10^{12}$	192	<b>410</b>	8
	0.1	3	1	3.42	$7.5 \times 10^{11}$	64	<b>160</b>	8
980703...	0.08	2	1	0.966	$2.7 \times 10^{10}$	69	<b>140</b>	8
	0.02	3	1	0.966	$8.0 \times 10^9$	24	<b>56</b>	8
990510...	0.1	2	1	1.62	$1.2 \times 10^{11}$	98	<b>200</b>	8
	0.03	3	1	1.62	$3.7 \times 10^{10}$	34	<b>79</b>	8
Unusual Bursts								
980425...	0.04	2	1	0.0085	$1.0 \times 10^4$	4.6	<b>6.4</b>	8
	0.01	3	1	0.0085	$2.9 \times 10^3$	2.8	<b>3.8</b>	8

Minimum Lorentz factors for the burst to be optically thin to pair production and to avoid scattering by pairs.

Lithwick & Sari, ApJ, 555, 540, (2001)

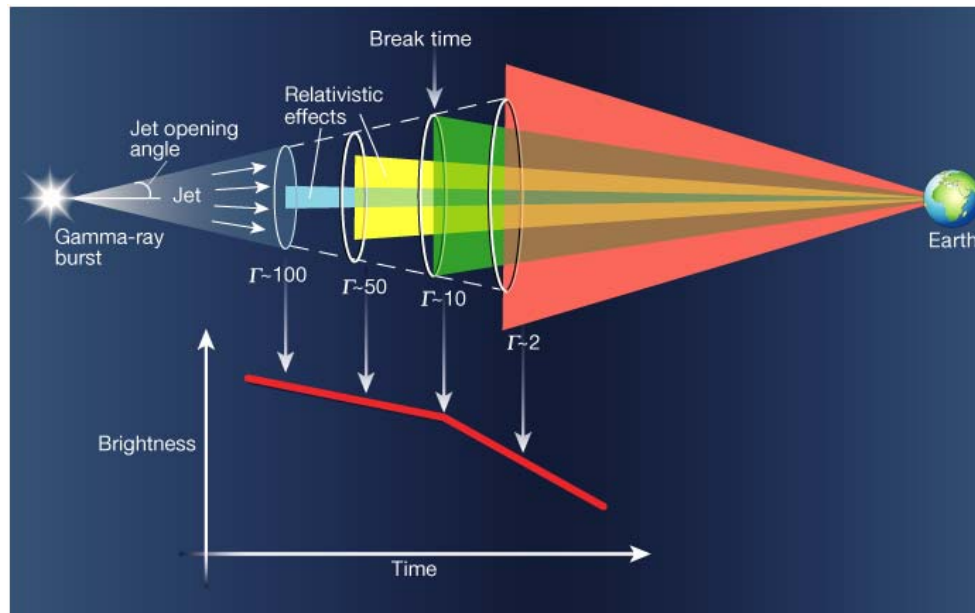
$$\Gamma \geq 200$$

It is a property of matter moving close to the speed of light that it emits its radiation in a small angle along its direction of motion. The angle is inversely proportional to the *Lorentz factor*

$$\Gamma = \frac{1}{\sqrt{1 - v^2 / c^2}}, \quad \text{E.g., } \Gamma = 100 \quad v = 0.99995 c$$

$$\theta = 1 / \Gamma \quad \Gamma = 10 \quad v = 0.995 c$$

This offers a way of measuring the beaming angle. As the beam runs into interstellar matter it slows down. At some point the luminosity begins to decline more quickly



Measurements give an opening angle of about 5 degrees.

- GRBs have total energies not too unlike supernovae

20

Frail et al. ApJL, (2001), astro/ph 0102282

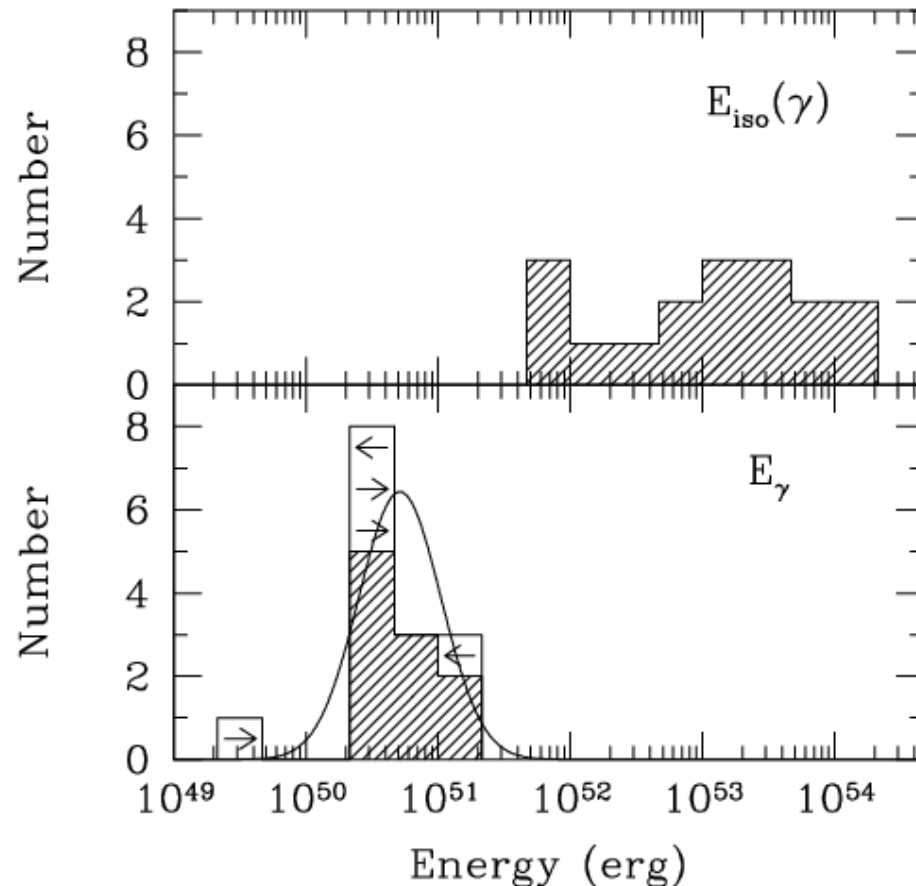


**Figure 3.** The distribution of the apparent isotropic  $\gamma$ -ray burst energy of GRBs with known redshifts (top) versus the geometry-corrected energy for those GRBs whose afterglows exhibit the signature of a non-isotropic outflow (bottom). The mean isotropic equivalent energy  $\langle E_{\text{iso}}(\gamma) \rangle$  for 17 GRBs is  $110 \times 10^{51}$  erg with a  $1\text{-}\sigma$  spreading of a multiplicative factor of 6.2. In estimating the mean geometry-corrected energy  $\langle E_{\gamma} \rangle$  we applied the Bayesian inference formalism<sup>60</sup> and modified to handle datasets containing upper and lower limits.<sup>61</sup> Arrows are plotted for five GRBs to indicate upper or lower limits to the geometry-corrected energy. The value of  $\langle \log E_{\gamma} \rangle$  is  $50.71 \pm 0.10$  ( $1\sigma$ ) or equivalently, the mean geometry-corrected energy  $\langle E_{\gamma} \rangle$  for 15 GRBs is  $0.5 \times 10^{51}$  erg. The standard deviation in  $\log E_{\gamma}$  is  $0.31^{+0.09}_{-0.08}$ , or a  $1\text{-}\sigma$  spread corresponding to a multiplicative factor of 2.0.

Despite their large inferred brightness, it is increasingly believed that GRBs are **not inherently much more powerful than supernovae**.

From afterglow analysis, there is increasing evidence for a small "beaming angle" and a common total jet energy near  $3 \times 10^{51}$  erg (for a conversion efficiency of 20%).

See also: Freedman & Waxman, ApJ, 547, 922 (2001)

Bloom, Frail, & Sari AJ, 121, 2879 (2001)

Piran et al. astro/ph 0108033

Panaitescu & Kumar, ApJL, 560, L49 (2000)

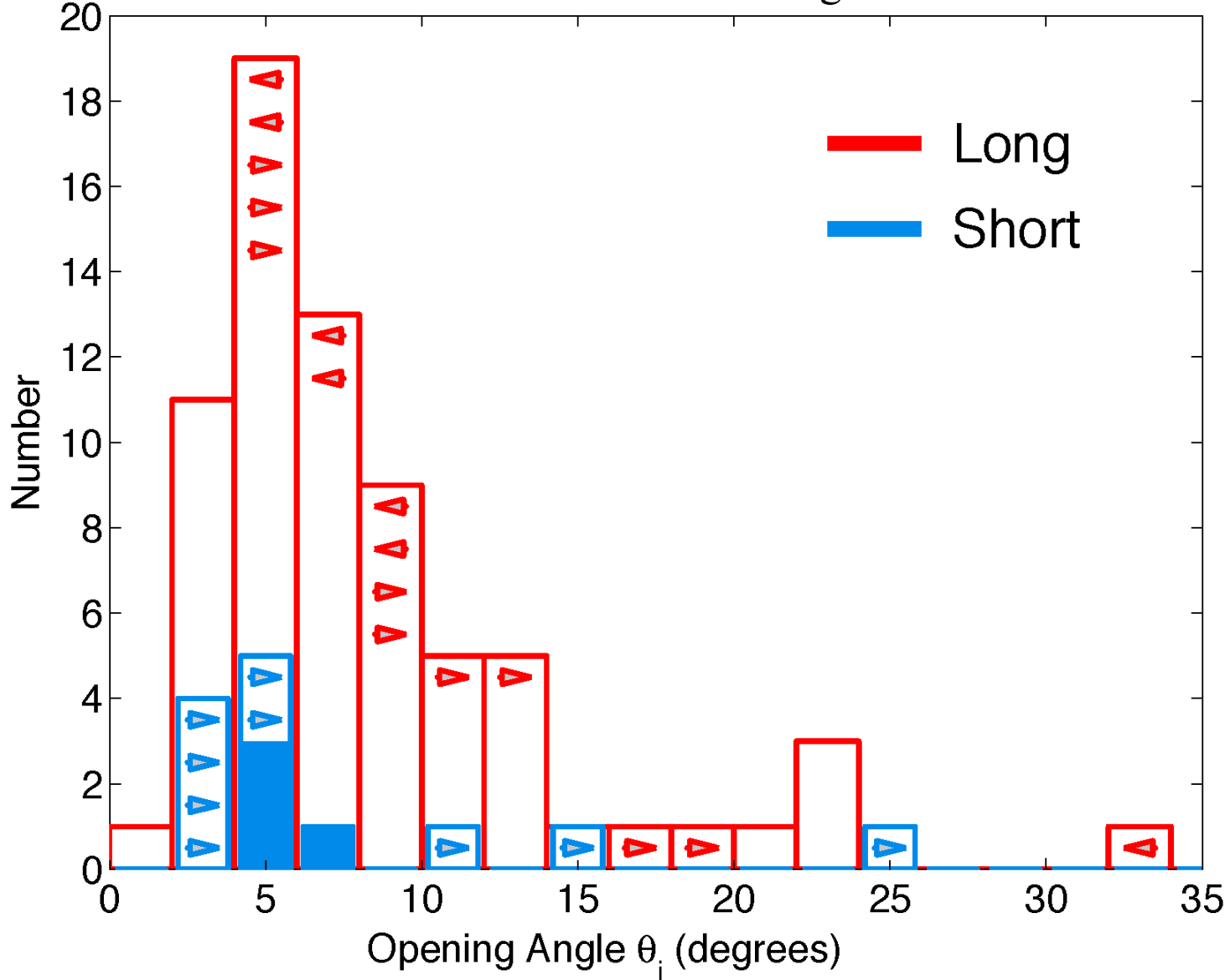
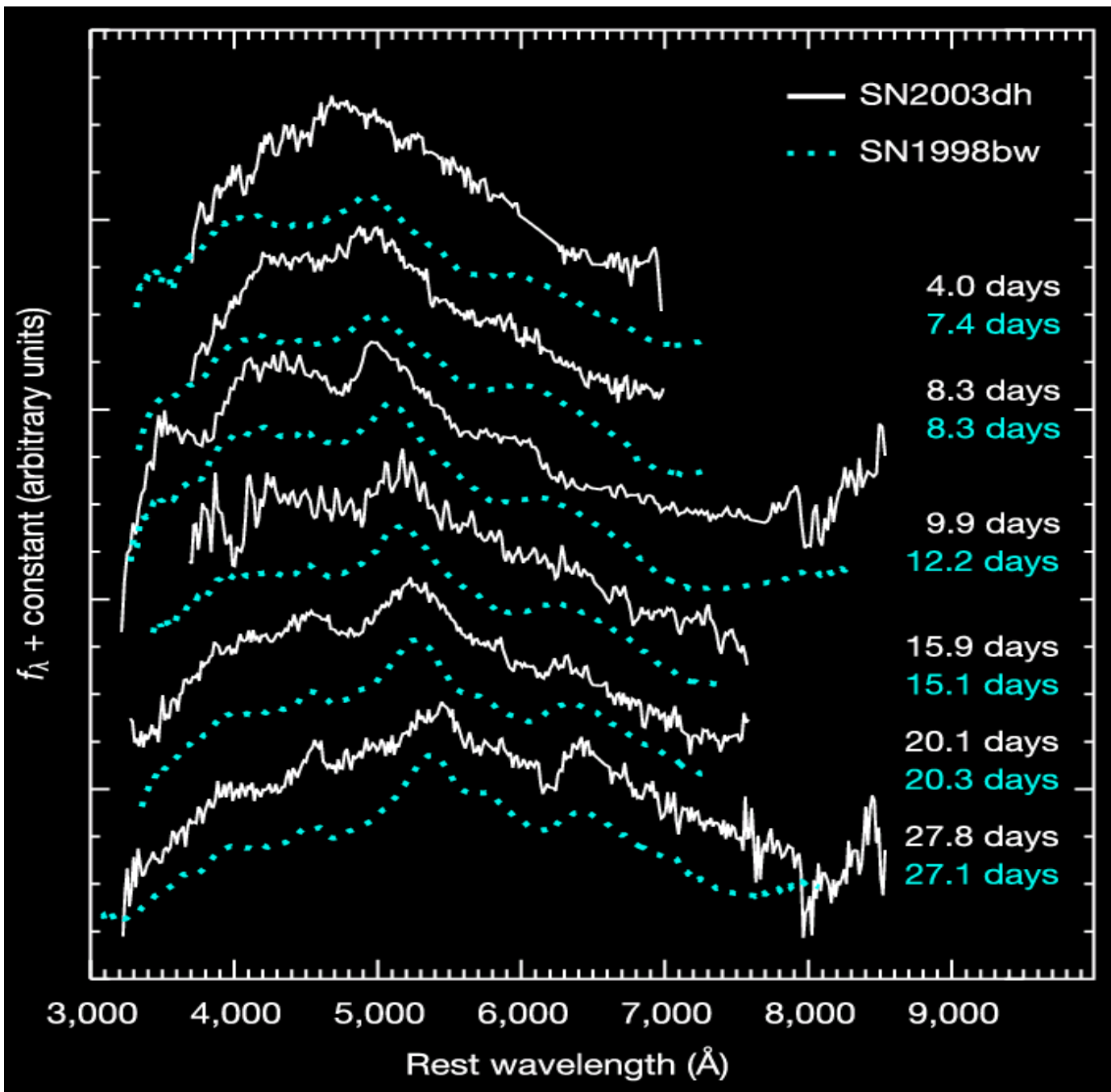


Figure 18:

Distributions of jet opening angles for short (blue) and long (red) GRBs, based on breaks in their afterglow emission. Arrows mark lower or upper limits on the opening angles. The observations are summarized in §8.4. From Fong et al. (2013) and references therein.



GRB980425/  
 SN1998bw

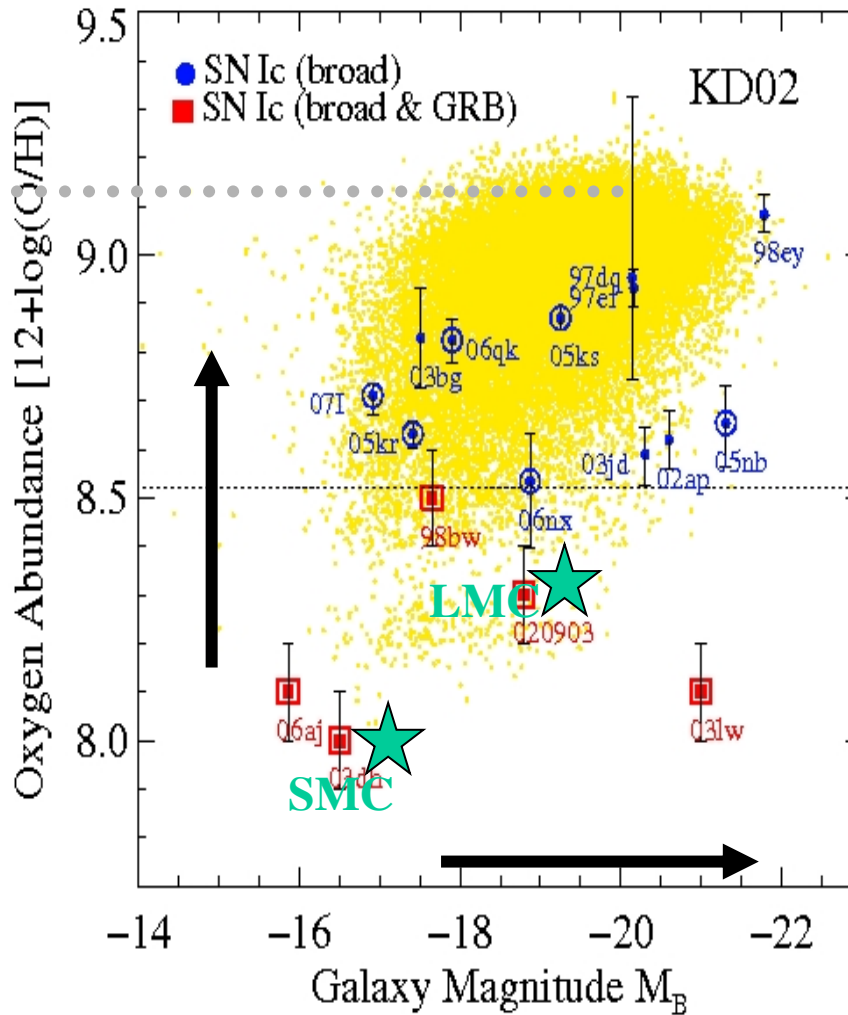
GRB030329/  
 SN2003dh

GRB031203/  
 SN2003lw

Hjorth et al. (2003),  
 Stanek et al. (2003)

# Local abundances of GRB-SN and broad-lined SN Ic

Local SDSS  
galaxies  
(Tremonti et al  
2004)



Modjaz et al (2008)

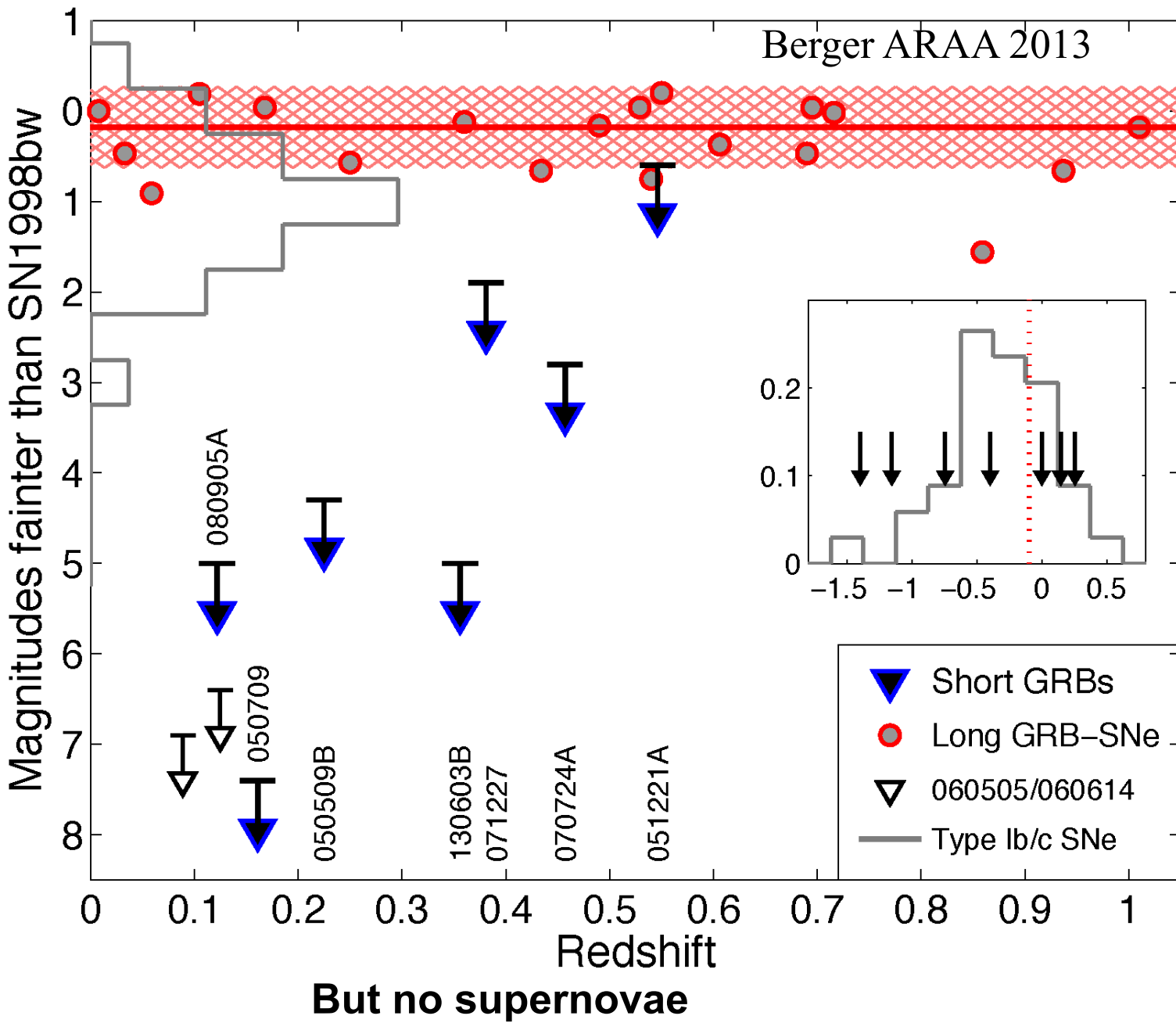


**Figure 2:**

Limits on supernovae associated with short GRBs (filled triangles) relative to the peak absolute magnitude of the canonical long GRB-SN 1998bw. Also shown are the distribution of SN peak magnitudes for long GRBs (filled circles; hatched region marks the median and standard deviation for the population; [Hjorth](#)

" **How common are SN Ib/c? Local rate:**

- ~15-20% of all SN
- ~30% of CC-SN
- Broad-lined SN Ic (SN Ic-BL): ~5-10% of all SN Ib/c

(Cappellaro et al 1999, Guetta & Della Valle 2007, Leaman et al. in prep)

So **SN Ic-BL are 1 - 2% of all supernovae.**

GRBs are a much smaller fraction. The distinction may be the speed of core rotation at death (which is correlated with the metallicity)

Not all SN Ic - BL are GRBs  
(though they may all be “active” at some level.

*The rate at which massive stars die in the universe is very high and GRBs are a small fraction of that death rate.*

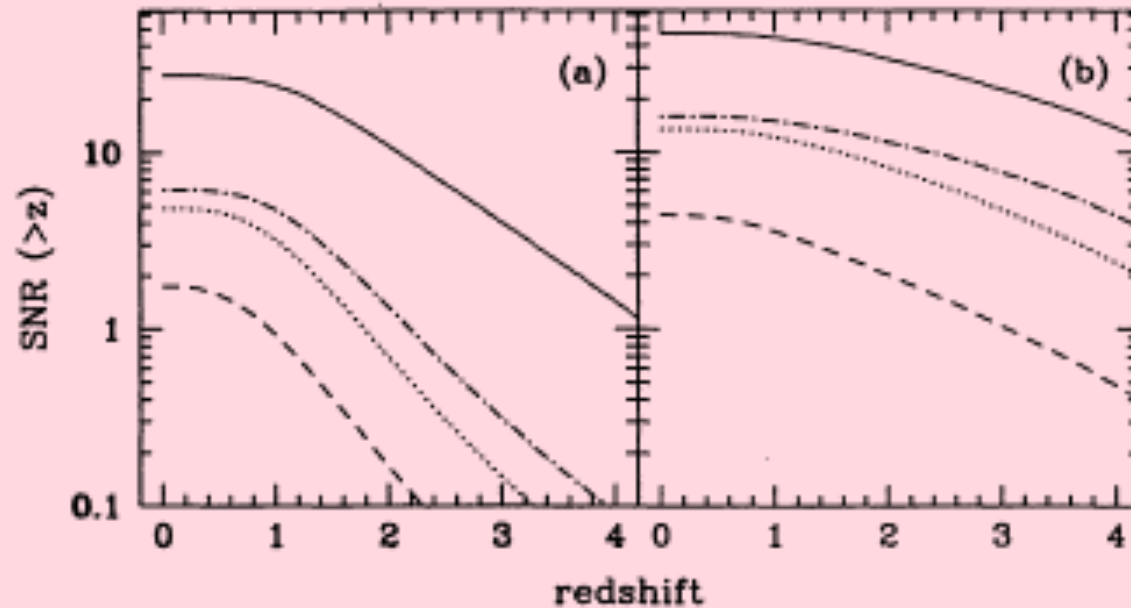


**Figure 3.** Predicted cumulative number of Type Ia and II(+b/c) SNe above a given redshift  $z$  in a  $4 \times 4$  arcmin<sup>2</sup> field. Solid line: Type II SNe. Dashed-dotted line: Type Ia SNe with  $\tau = 0.3$  Gyr. Dotted line: Type Ia SNe with  $\tau = 1$  Gyr. Dashed line: Type Ia SNe with  $\tau = 3$  Gyr. The effect of dust extinction on the detectability of SNe is negligible in these models. (a) Model predictions of the 'merging' scenario of Fig. 1a. (b) Same for the 'monolithic collapse' scenario of Fig. 1b.

Madau, della Valle, & Panagia, MNRAS, 1998

Supernova rate per 16 arc min squared per year  
 $\sim 20$

*This corresponds to an all sky supernova rate of*

*6 SN/sec*

*For comparison the universal GRB rate is about 3 /day \* 300 for beaming or*

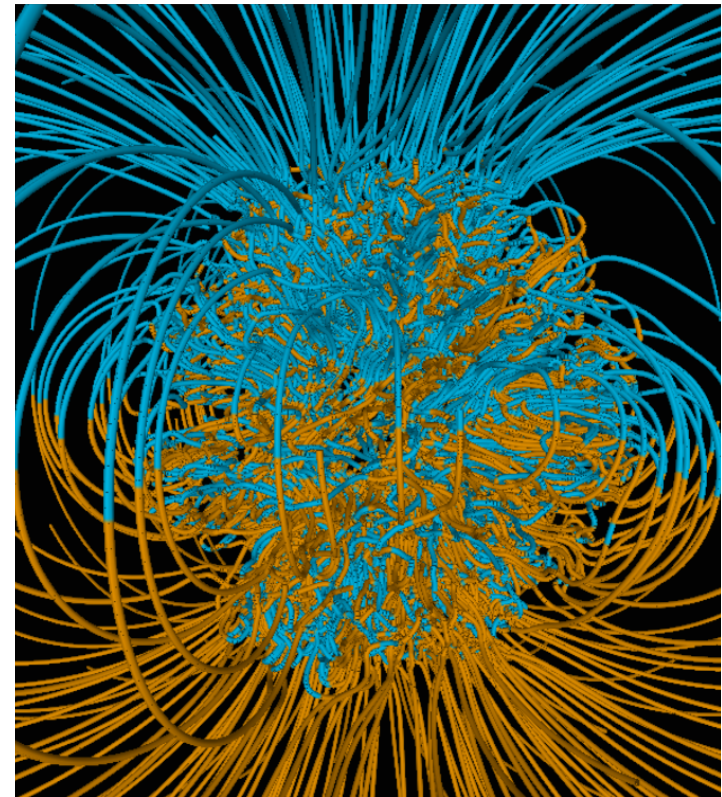
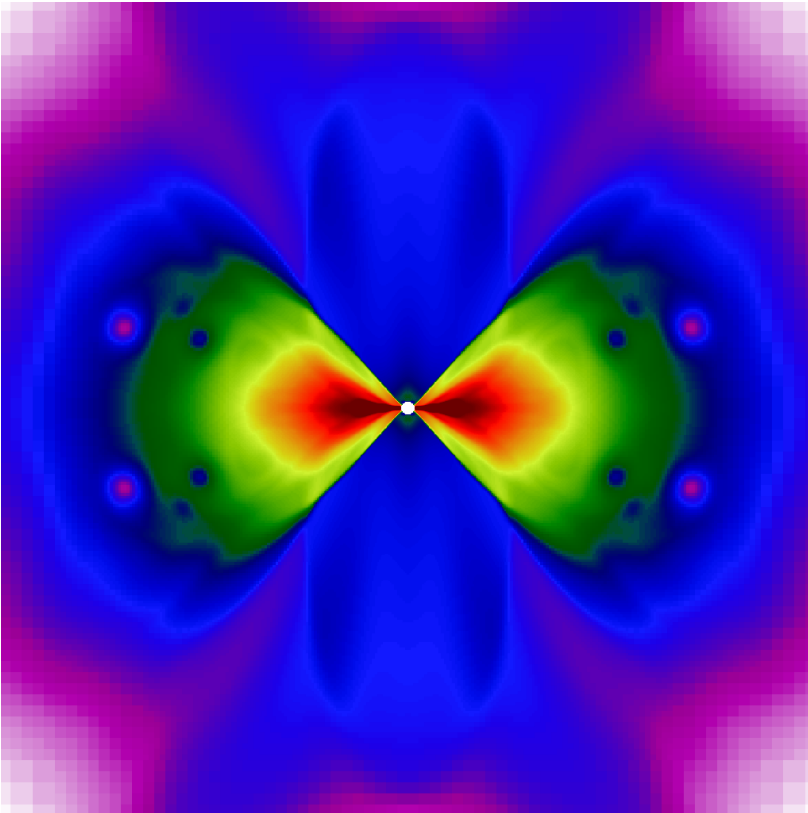
*$\sim 0.02$  GRB/sec*

# *Models*

It is the consensus that the root cause of these energetic phenomena is star death that involves an unusually large amount of angular momentum ( $j \sim 10^{16} - 10^{17} \text{ cm}^2 \text{ s}^{-1}$ ) and quite possibly, one way or another, ultra-strong magnetic fields ( $\sim 10^{15}$  gauss). These are exceptional circumstances. A neutron star or a black hole is implicated.

*Today, there are two principal models being discussed for GRBs of the “long-soft” variety:*

- The collapsar model
- The millisecond magnetar



The ultimate source of energy in both is rotation.

## “Predictions” of both the collapsar and magnetar models

### LSBs

- Relativistic jets 
- Occur in star forming regions 
- Occur in hydrogen-stripped stars and are often accompanied by SN Ibc 
- Are a small fraction of SN Ibc  ~0.3% of all SN
- Are favored by low metallicity (and rapid rotation) 

*Magnetar  
Model*

# Proto-magnetars

Magnetars have fields  $\sim 10^{14-15}$  G  
 They might be born as fast rotators  
 Efficient dynamo implies  $P \sim t_{\text{conv}} \sim \text{ms}$

Millisecond magnetar have the correct energy  

$$E_{\text{Rot}} \approx 2 \times 10^{52} \left( \frac{P}{1 \text{ ms}} \right)^{-2} \text{ ergs}$$

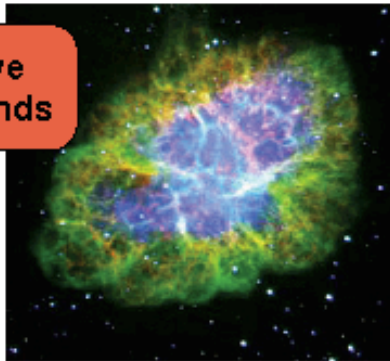
*Pro*

NS are naturally associated to core collapse SN  
 Less angular momentum required than BH-AD  
 NS population can explain transition from asymmetric SNe to XRFs to GRBs

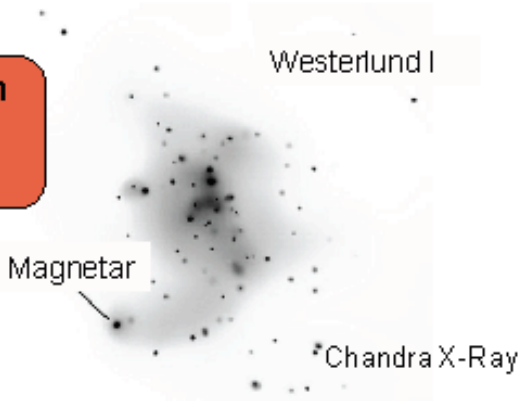
Typical spin-down times are  $\sim 100-1000$  sec  

$$\dot{E} \approx 10^{49} \left( \frac{P}{1 \text{ ms}} \right)^{-4} \left( \frac{B_{\text{Dip}}}{10^{15} \text{ G}} \right)^2 \text{ ergs s}^{-1}$$

Pulsars have relativistic winds



Magnetars can have massive progenitors



Faintest Cluster Members are O7 (Muno 2006)

Bucciantini, Quataert, Arons, Metzger and Thompson (MNRAS; 2007) and refs therein, see also Komissarov et al (2008)

Assume a pre-existing supernova explosion in the stripped down core of a 35 solar mass star.

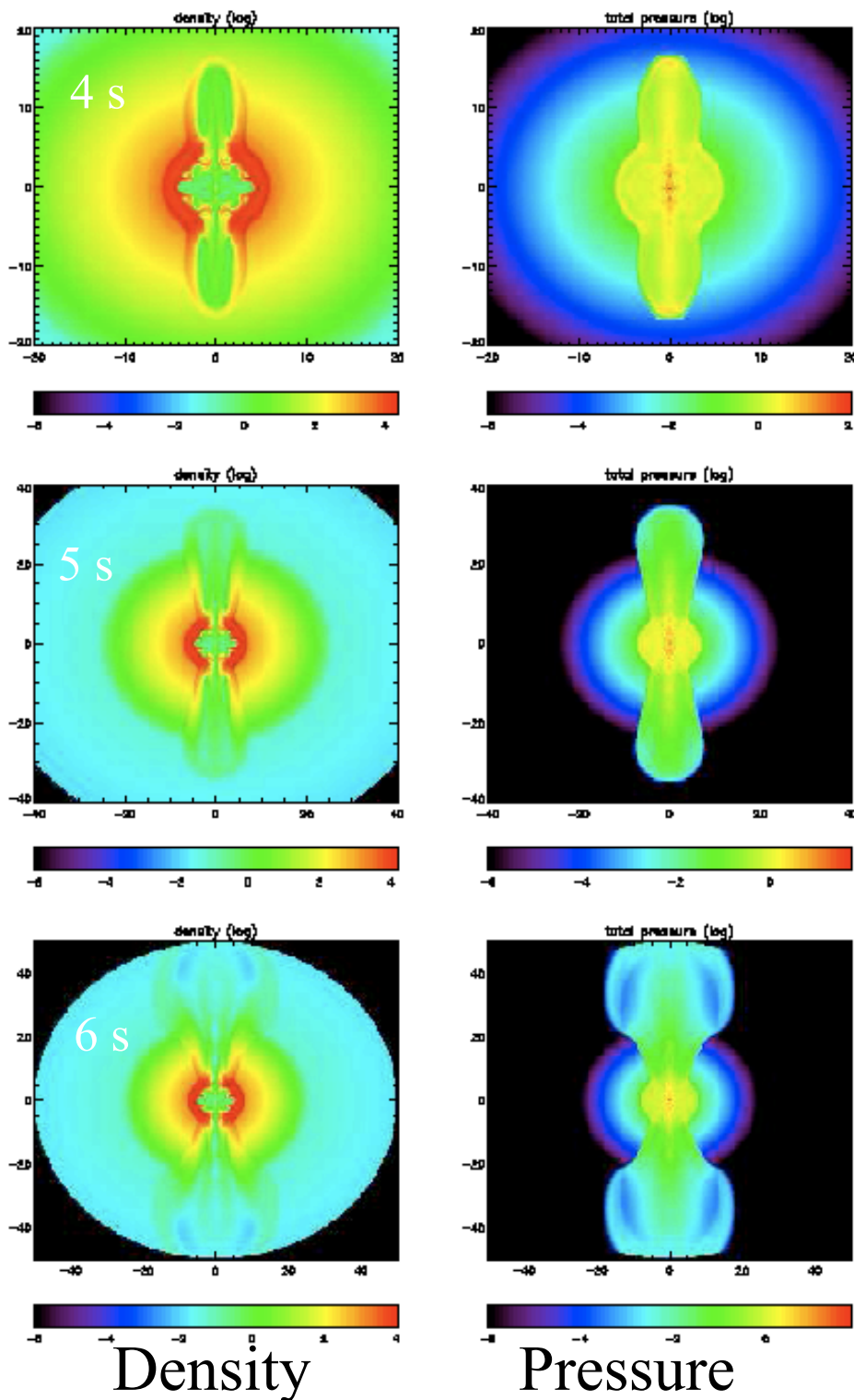
Insert a spinning down 1 ms magnetar with  $B \sim \text{few} \times 10^{15}$  gauss.

Two phase wind:

Initial magnetar-like wind contributes to explosion energy. Analog to pulsar wind. Sub-relativistic

Later magnetically accelerated neutrino powered wind with wound up B field makes jet. Can achieve high field to baryon loading.

*See especially Metzger et al (2011; MNRAS 413, 2031)*



The maximum energy available for the supernova and the GRB producing jet in the magnetar model is  $\sim 2 \times 10^{52}$  erg.

Consistent with observed limits of  $E_{\text{GRB}} + E_{\text{SN}}$  (Mazzali et al, 2014, *MNRAS*, **443**, 67)

Total rotational kinetic energy for a neutron star

$$E_{\text{rot}} \sim 2 \times 10^{52} (1 \text{ ms}/P)^2 (R/10 \text{ km})^2 \text{ erg}$$

This is the maximum value for a cold, rigidly rotating neutron star. A proto-neutron star at 10 - 100 ms is neither. Its large entropy makes the radius bigger and  $E_{\text{rot}}$  less, differential rotation increases  $E_{\text{rot}}$ . The trade off means that the above limit is not far off. Detailed calculations needed but consistent with Burrows et al.

## Major Uncertainties

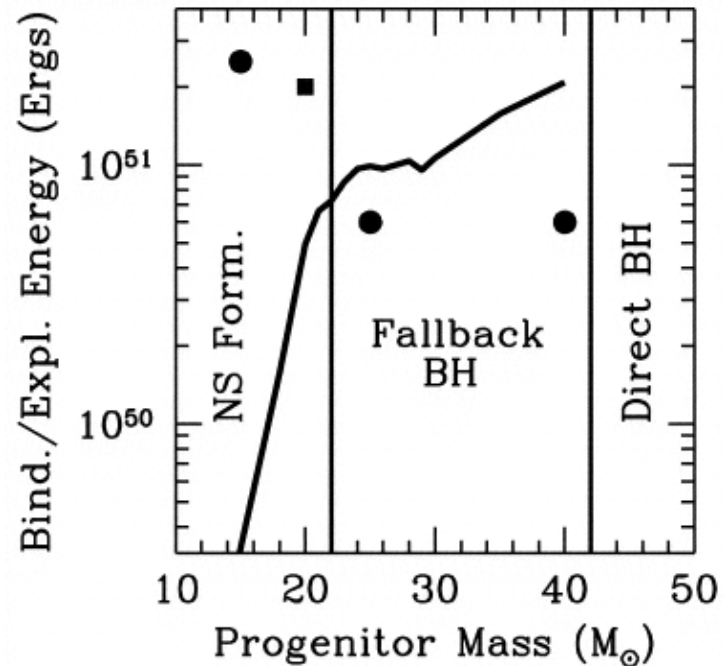
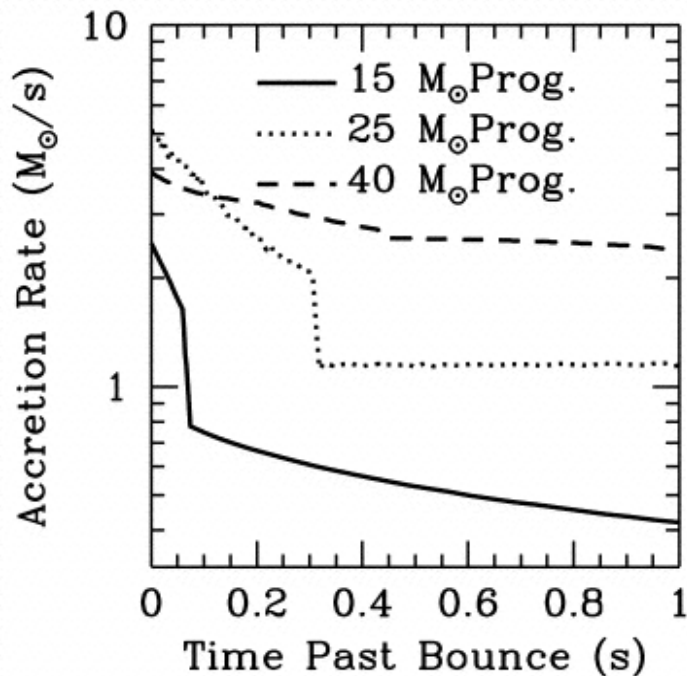
- What launches the supernova that clears the matter away from the vicinity of the neutron star and allows it to operate as in a vacuum?
- What distinguishes magnetar birth from GRBs? Is it a continuum based on rotation rate?
- Can dipole fields of  $10^{16}$  G be realized?
- How is several tenths of a solar mass of  $^{56}\text{Ni}$  made?

*Collapsar  
Model*

# Collapsar Progenitors

## Two requirements:

- **Core collapse produces a black hole** - either promptly or very shortly thereafter.
- **Sufficient angular momentum** exists to form a disk outside the black hole (this virtually guarantees that the hole is a Kerr hole)



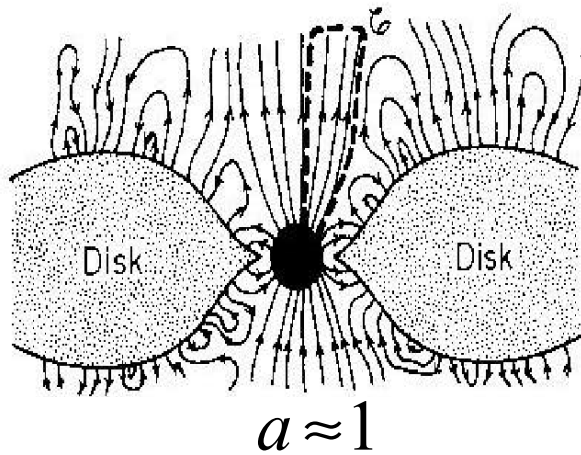
For the last stable orbit around a black hole in the collapsar model (i.e., the minimum  $j$  to make a disk)

$$j_{LSO} = 2\sqrt{3} GM / c = 4.6 \times 10^{16} M_{BH} / 3 M_{\odot} \text{ cm}^2 \text{ s}^{-1} \quad \text{non-rotating}$$

$$j_{LSO} = 2 / \sqrt{3} GM / c = 1.5 \times 10^{16} M_{BH} / 3 M_{\odot} \text{ cm}^2 \text{ s}^{-1} \quad \text{Kerr } a = 1$$

$$j_{ms\ magnetar} \approx \omega R^2 = \frac{2\pi}{.001} (1.1 \times 10^6)^2 = 7 \times 10^{15} \text{ cm}^2 \text{ s}^{-1}$$

*It is somewhat easier to produce a magnetar model!*



## MHD Energy Extraction

*Blandford & Znajek (1977)*  
*Komissarov and Barhov (2009)*  
*etc.*

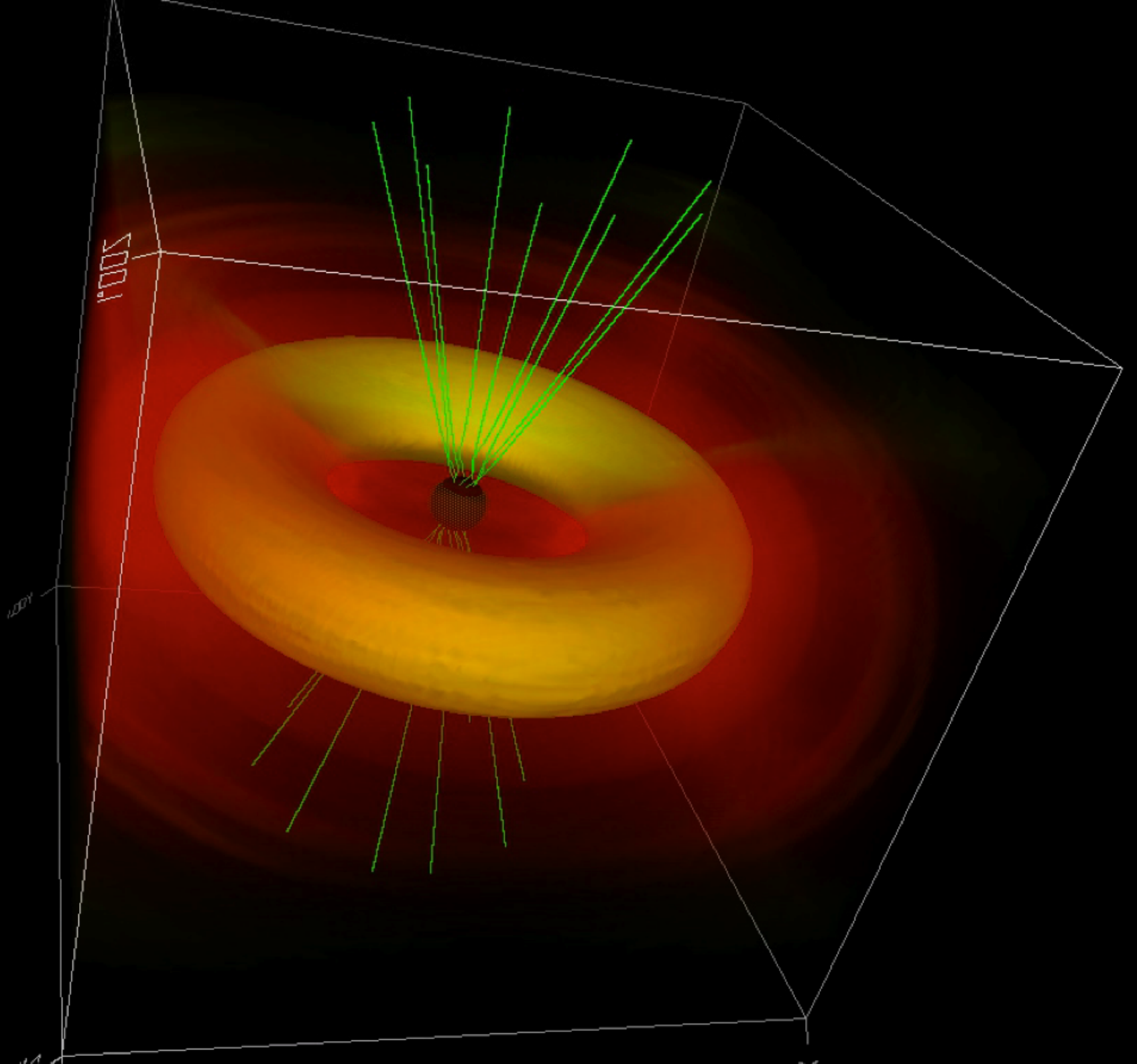
From the rotational energy of the black hole:

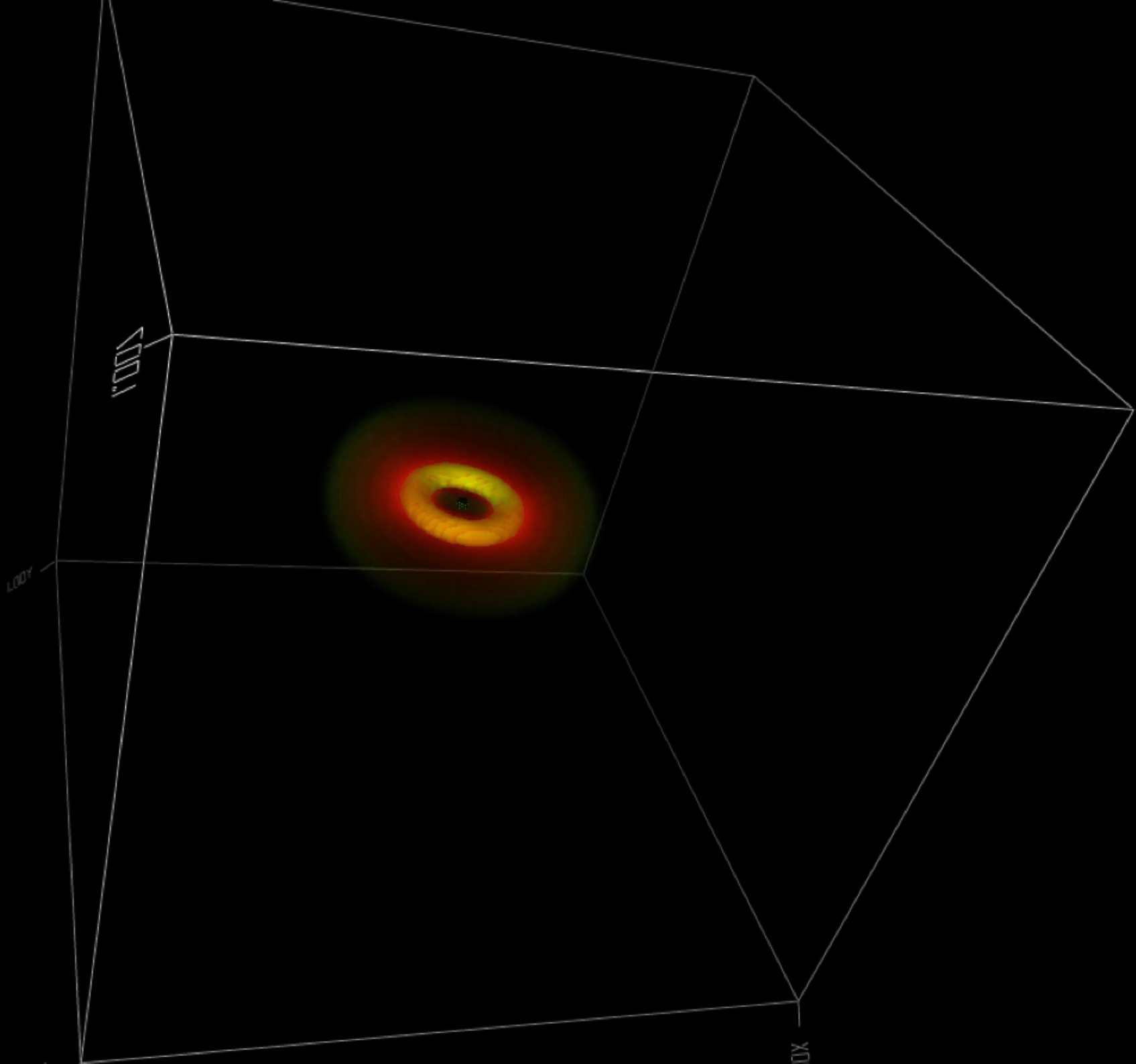
$$L_{BZ} \sim 4 \times 10^{50} B_{15}^2 a^2 \left( \frac{M}{M_{\odot}} \right)^2 \text{ erg s}^{-1}$$

for an efficiency factor  $\sim 0.03$  (see previous lecture).  $M \sim 3 - 10 M_{\odot}$

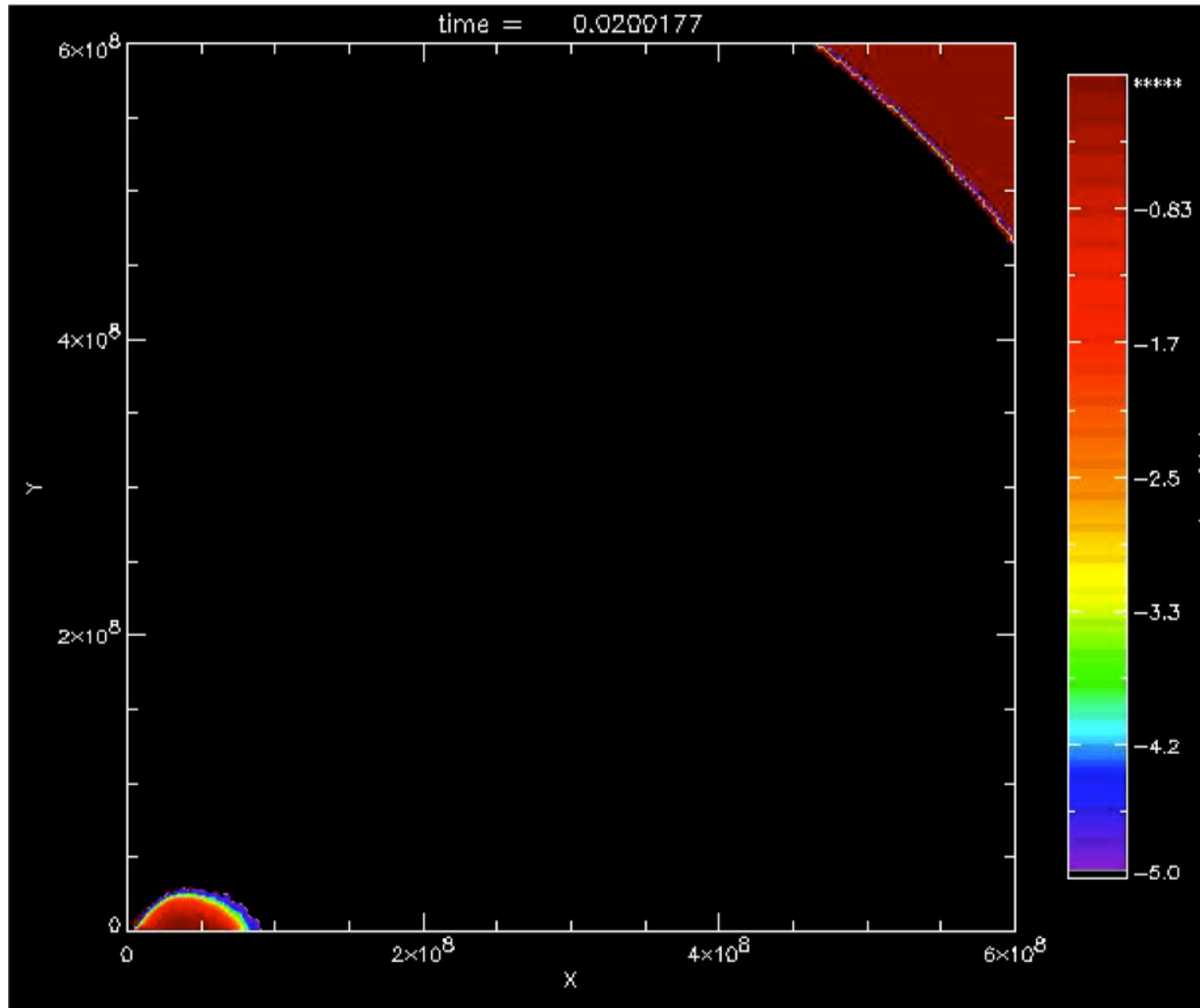
The efficiencies for converting accreted matter to energy need not be large.  $B \sim 10^{14} - 10^{15}$  gauss for a 3 solar mass black hole. Well below equipartition in the disk.

Eventually shuts off when  $\dot{M}$  can no longer sustain such a large B-field.





# The disk wind: MacFadyen & Woosley (2001)

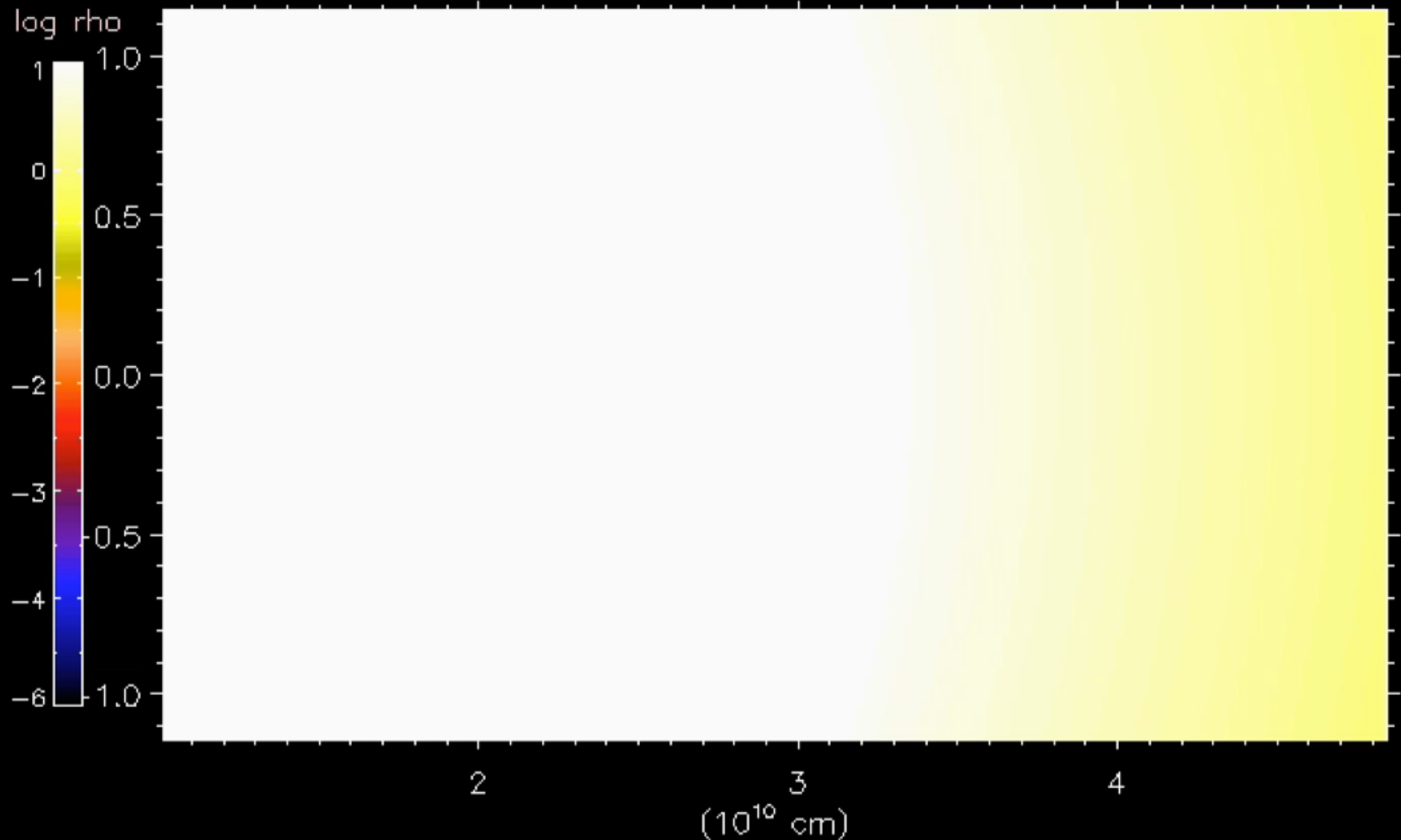


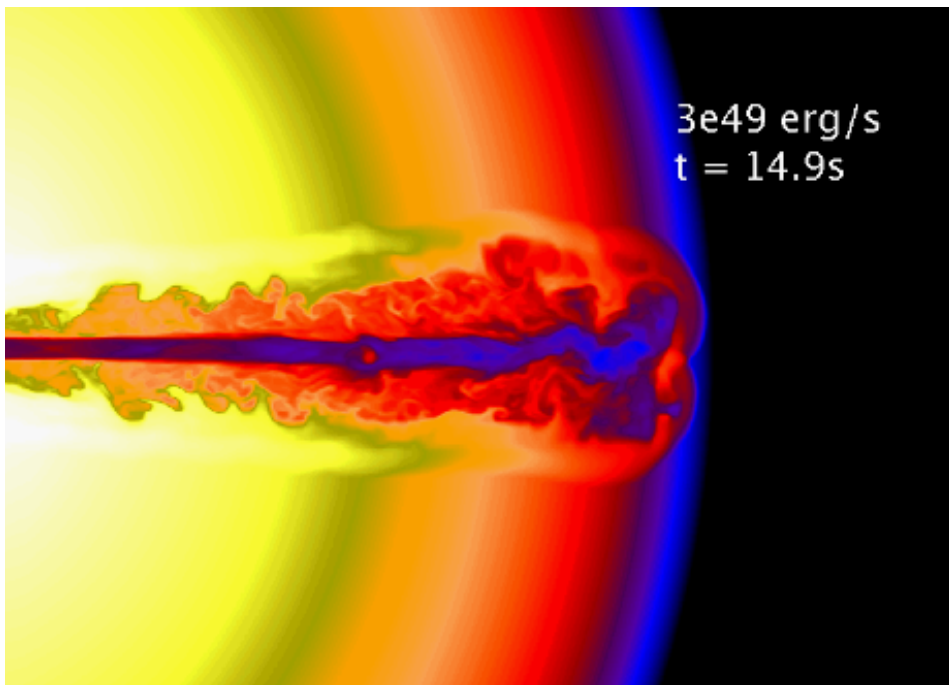
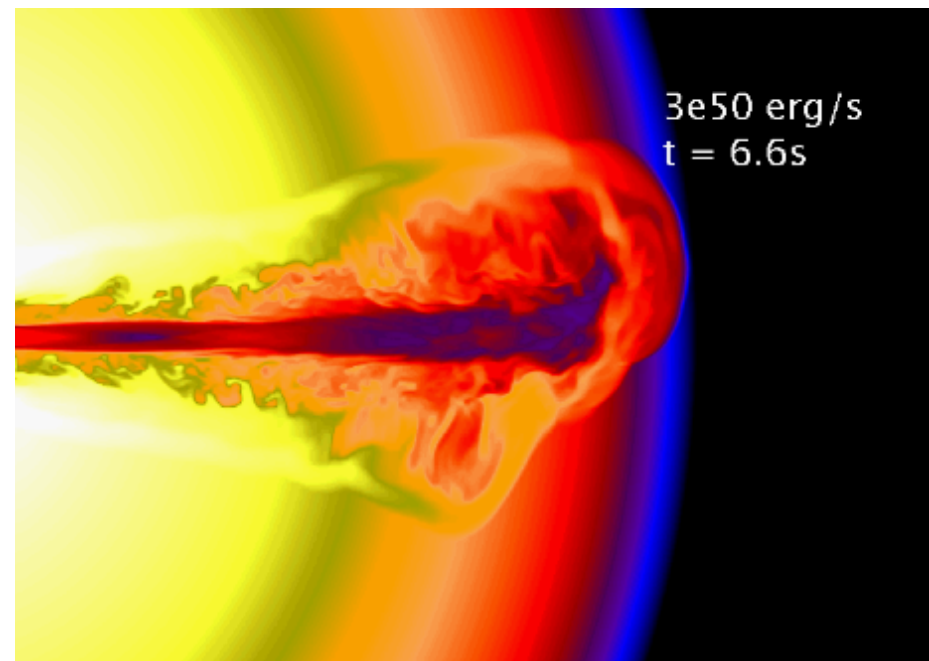
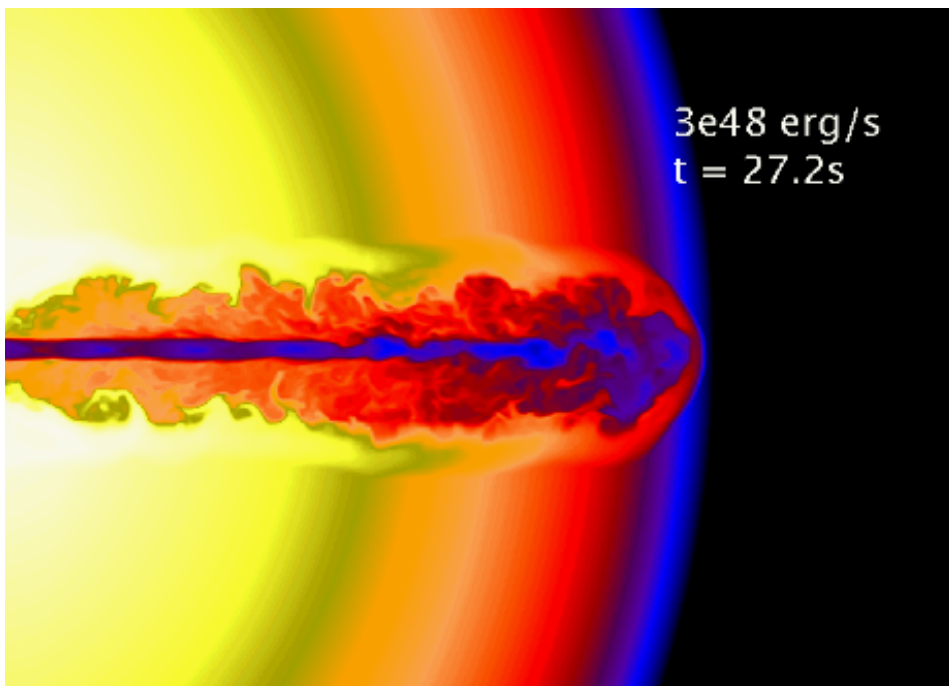
# 3-D Special Relativistic Hydro Simulation of Collapsar Jet

Wei-qun Zhang, & S.E. Woosley

Model 3BL

$t = 0.00$  s





3D studies of relativistic jets  
by Woosley & Zhang (2007 and in prep.)

*As the energy of the jet is turned down at the origin, the jet takes an increasingly long time to break out. The cocoon also becomes smaller and the jet more prone to instability.*

Jets were inserted at  $10^{10}$  cm in a WR star with radius  $8 \times 10^{10}$  cm. Jets had initial Lorentz factor of 5 and total energy 40 times  $mc^2$ .

*How to Get  
the Necessary  
Rotation*

*Need iron core rotation at death to correspond to a pulsar of < 5 ms period if rotation and B-fields are to matter to the explosion. Need a period of ~ 1 ms to make GRBs. This is much faster than observed in common pulsars.*

Total rotational kinetic energy for a neutron star

$$E_{\text{rot}} \sim 2 \times 10^{52} (1 \text{ ms}/P)^2 (R/10 \text{ km})^2 \text{ erg}$$

$$j = R^2 \Omega \sim \boxed{6.3 \times 10^{15}} (1 \text{ ms}/P) (R/10 \text{ km})^2 \text{ cm}^2 \text{ s}^{-1} \text{ at } M \approx 1.4 M_{\odot}$$

For the last stable orbit around a black hole in the collapsar model (i.e., the minimum  $j$  to make a disk)

$$j_{\text{LSO}} = 2\sqrt{3} GM/c = \boxed{4.6 \times 10^{16}} M_{\text{BH}} / 3 M_{\odot} \text{ cm}^2 \text{ s}^{-1} \quad \text{non-rotating}$$

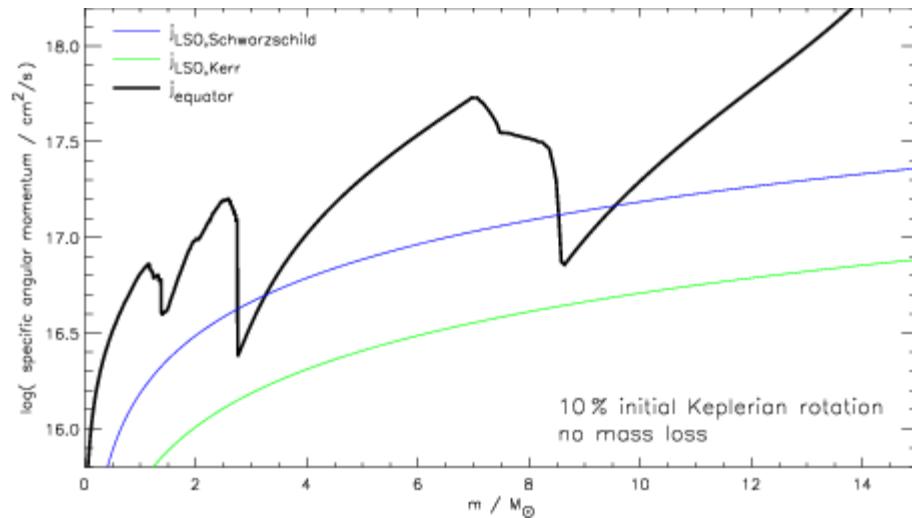
$$j_{\text{LSO}} = 2/\sqrt{3} GM/c = \boxed{1.5 \times 10^{16}} M_{\text{BH}} / 3 M_{\odot} \text{ cm}^2 \text{ s}^{-1} \quad \text{Kerr } a = 1$$

*It is easier to produce a magnetar model!*

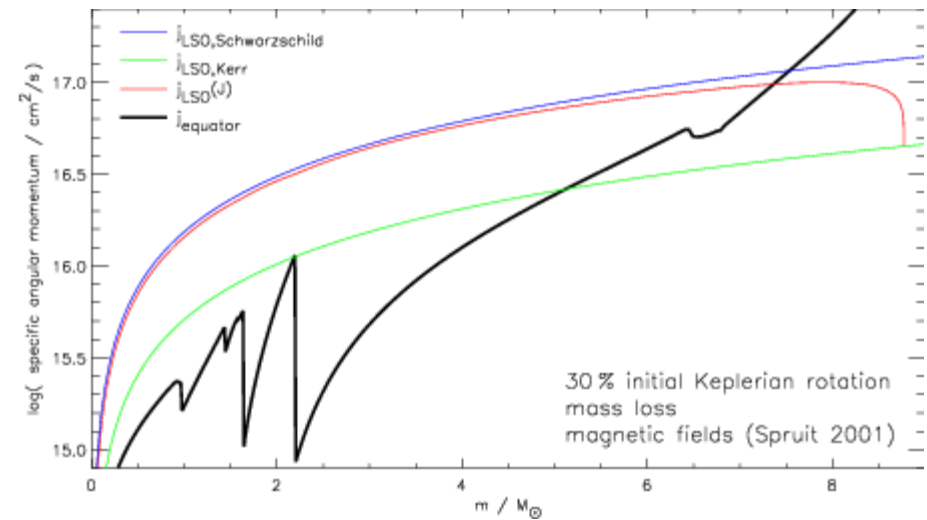
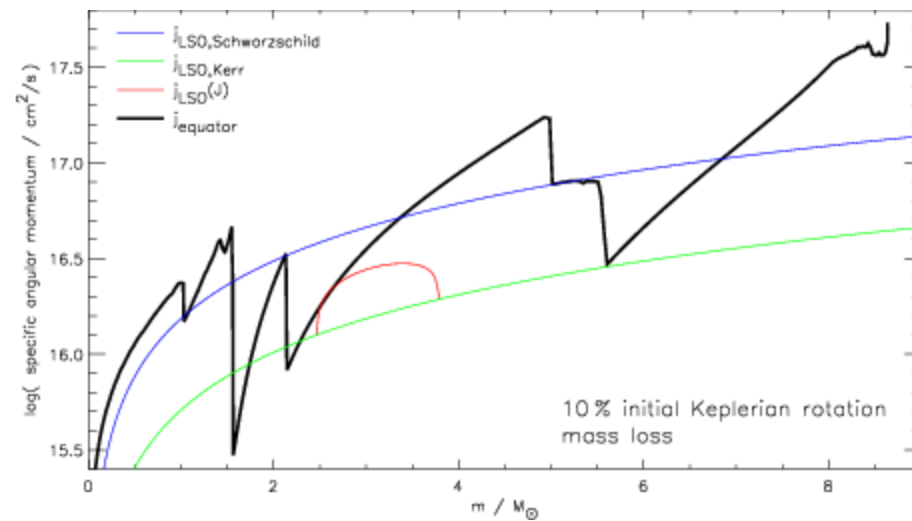
*The more difficult problem is the angular momentum. This is a problem shared by all current GRB models that invoke massive stars...*

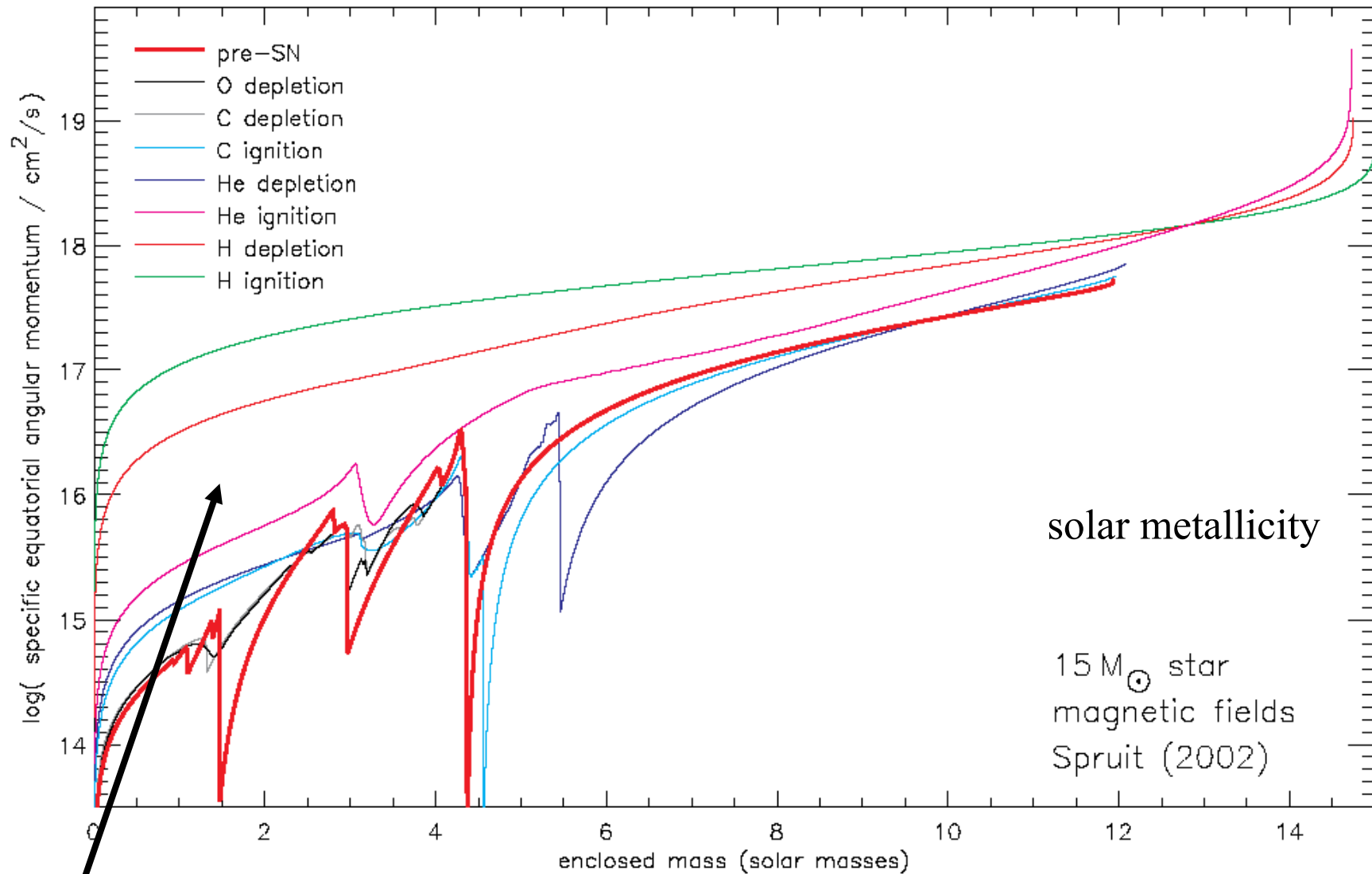
In the absence of mass loss and magnetic fields, there would be abundant progenitors.

Unfortunately nature has both.



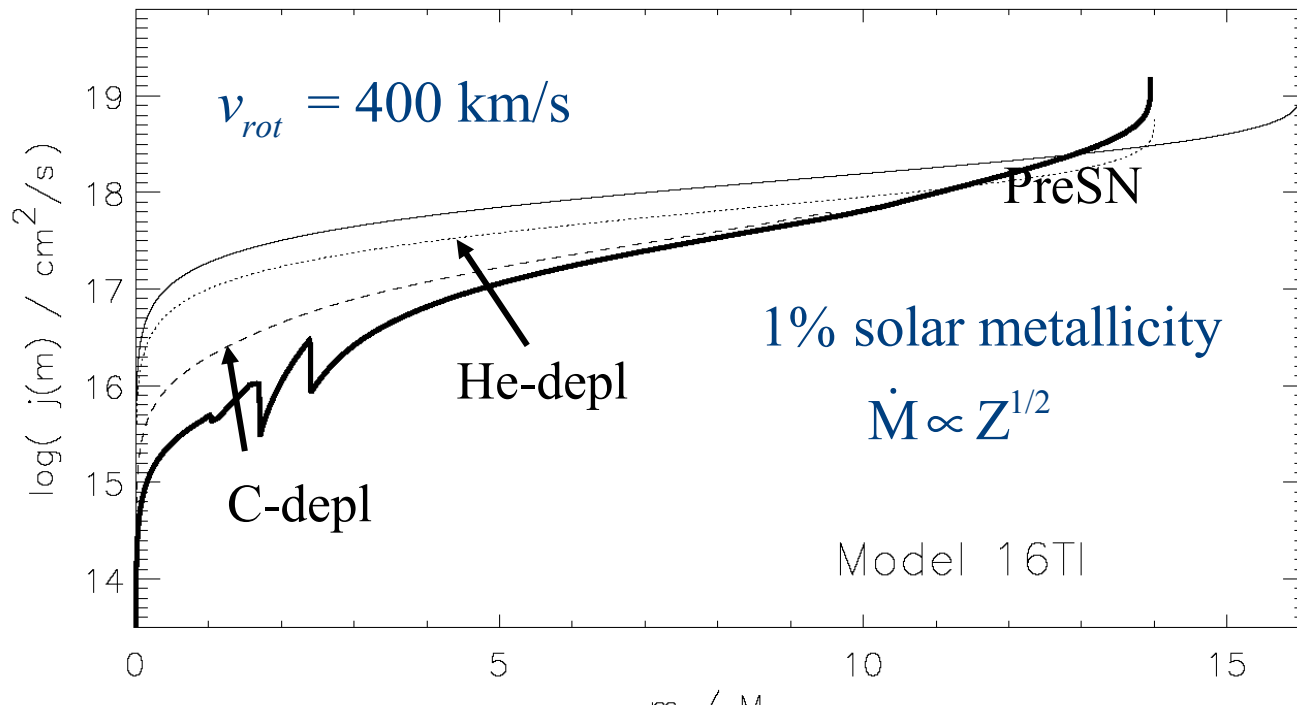
15 solar mass helium core born rotating rigidly at  $f$  times break up



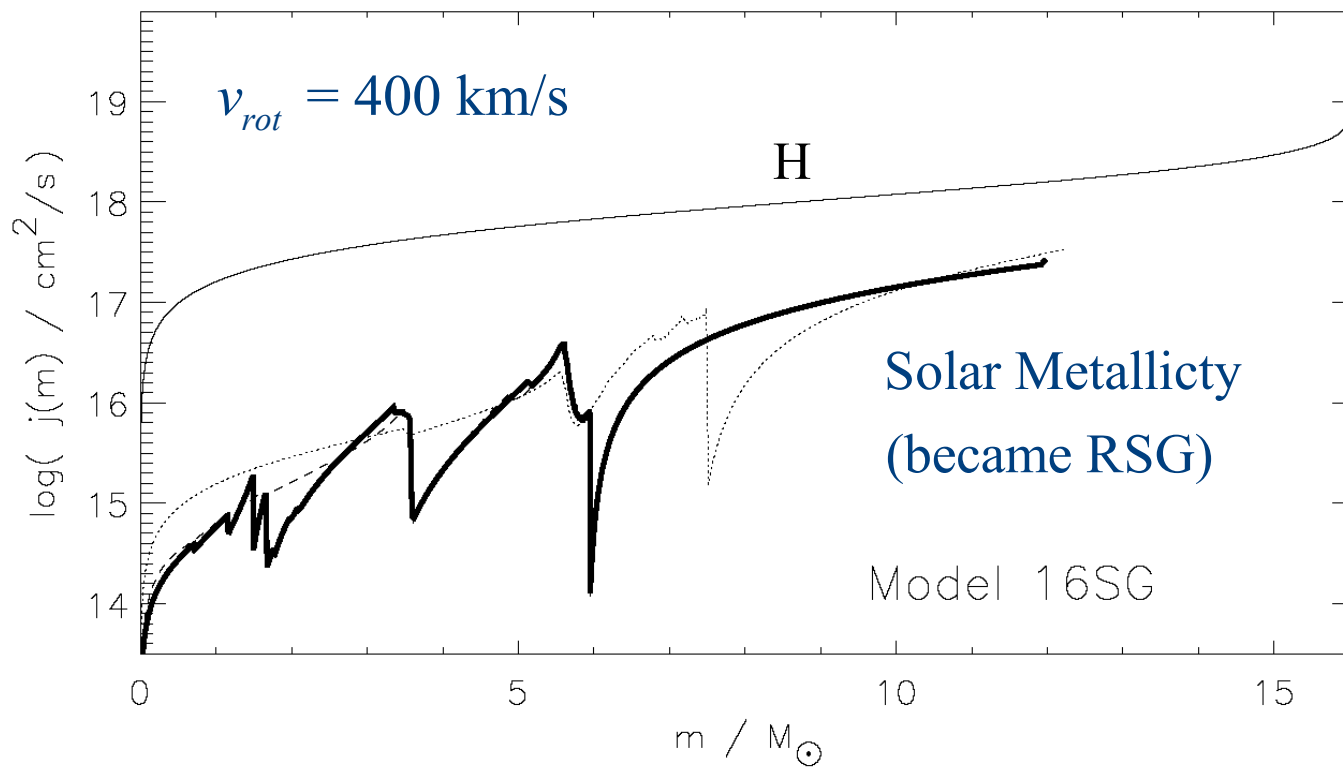


Much of the spin down occurs as the star evolves from H depletion to He ignition, i.e. forming a red supergiant.

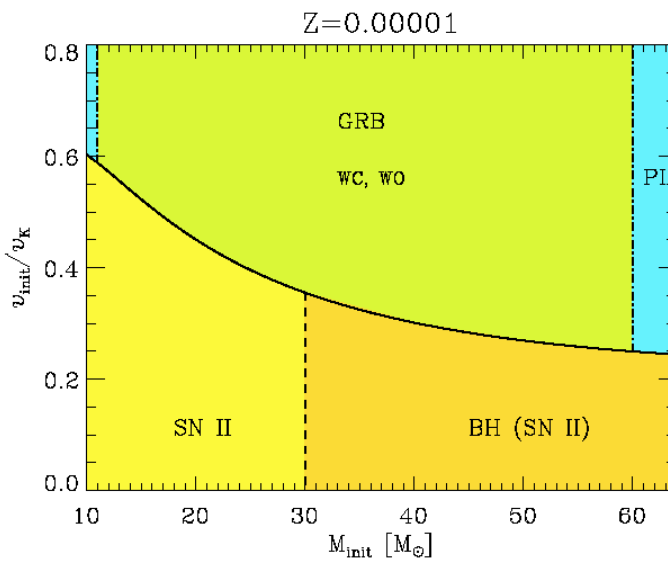
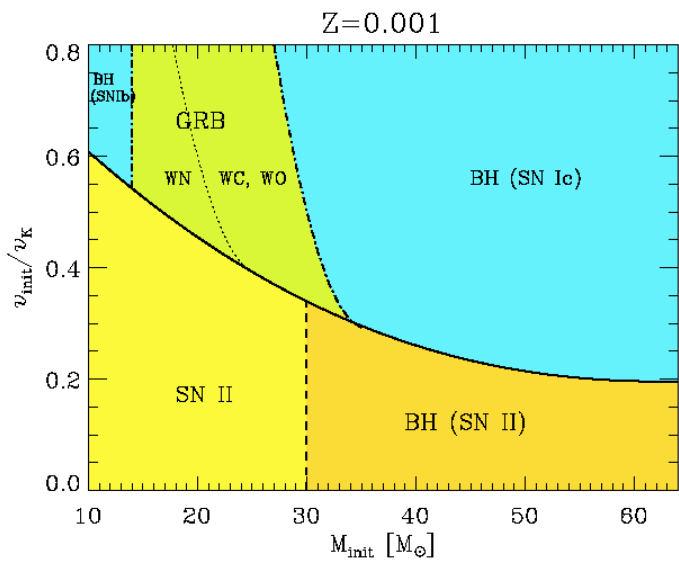
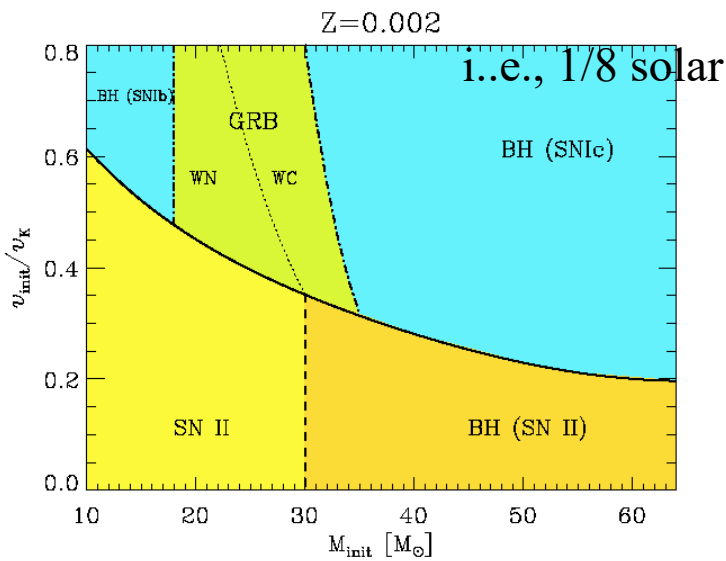
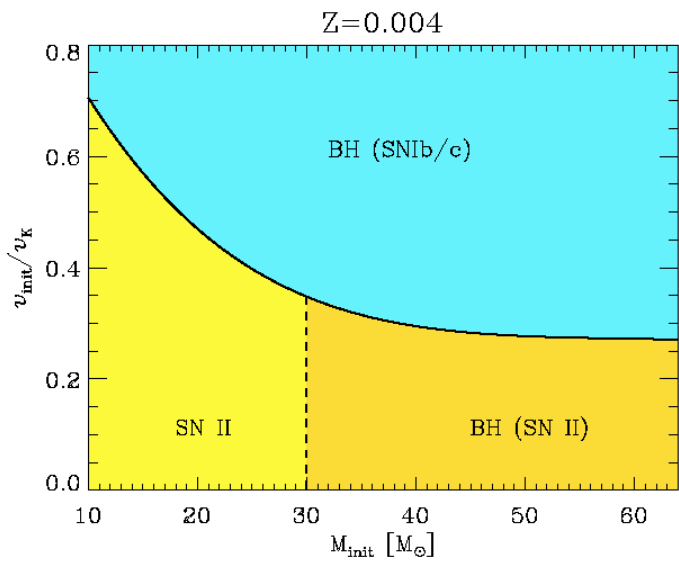
Heger, Woosley, & Spruit (2004)



GRB



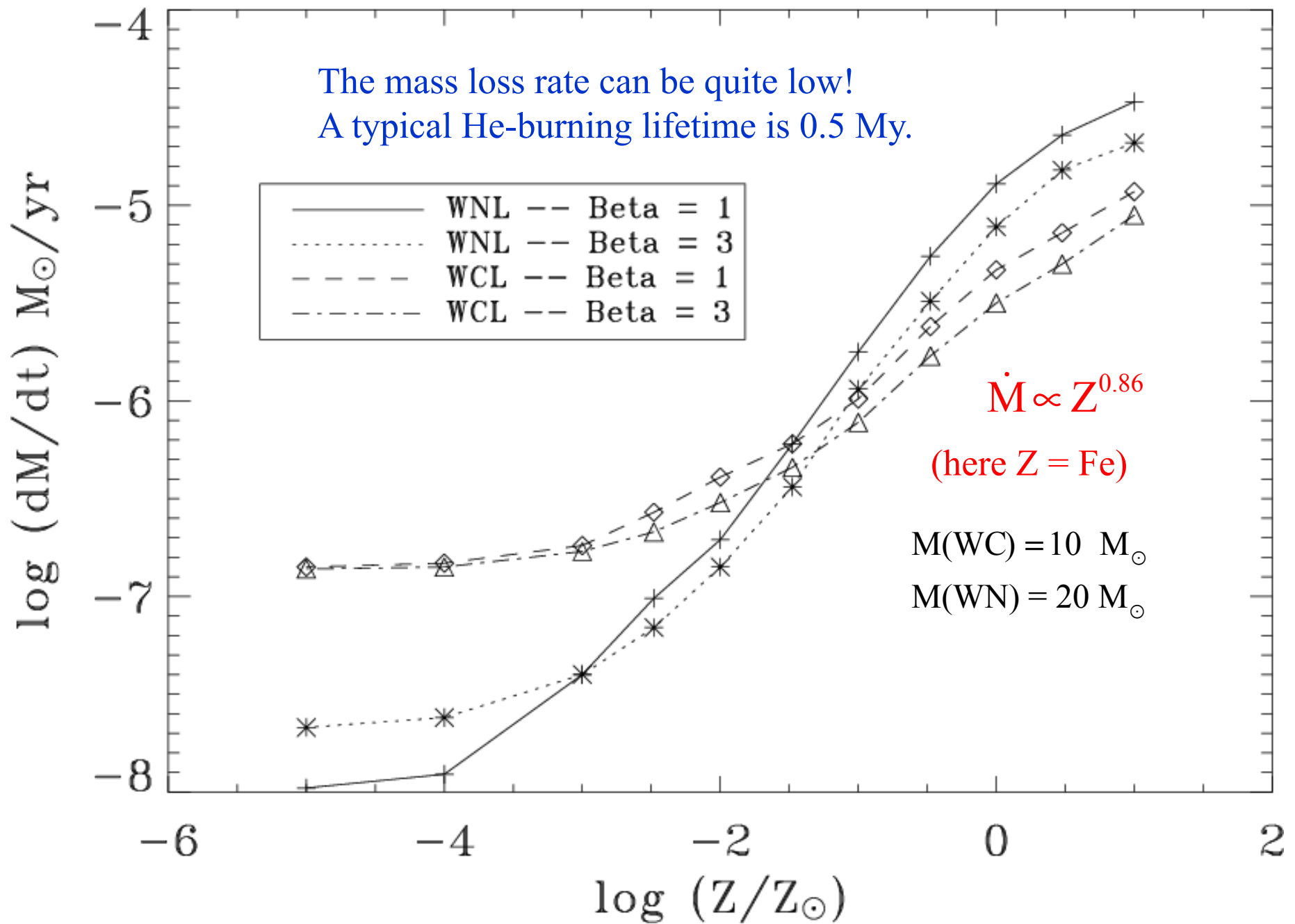
8 ms pulsar



Yoon, Langer,  
and Norman (2006)

$N_{GRB} / N_{SN} \ll 1\%$   
out to redshift 4  
saturates at 2% at  
redshift 10

Woosley and Heger (2006) find similar results but estimate a higher metallicity threshold (30% solar) and a higher mass cut off for making GRBs.



Theory

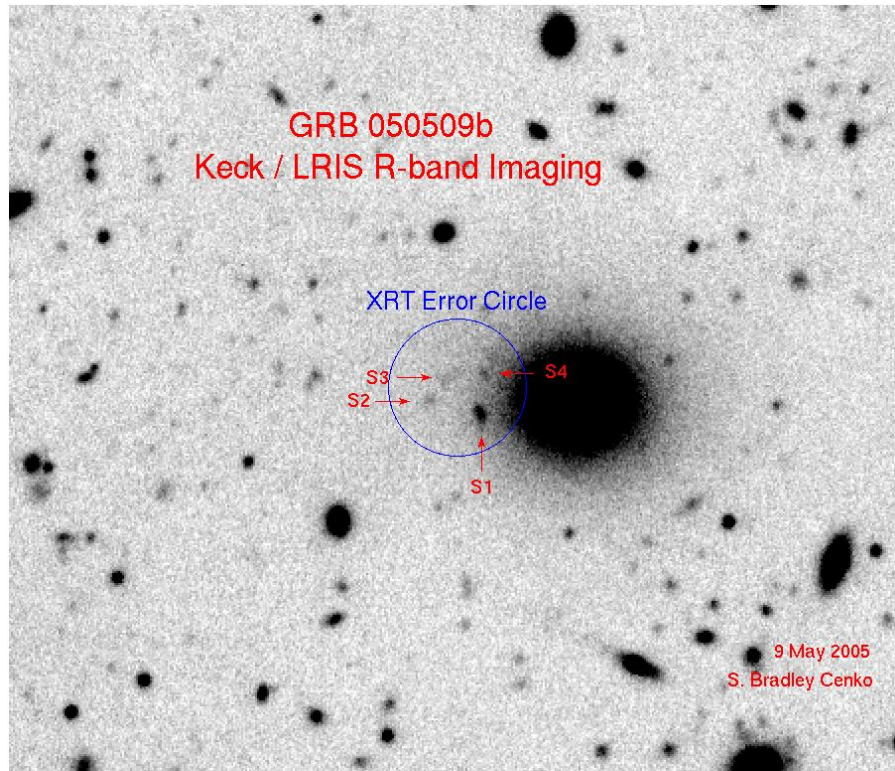
Vink & de Koter (A&A, 442, 587, (2005))

Savalio et al. (2009, ApJ, 691, 182) surveyed 46 GRB host galaxies. Found median mass to be  $10^{9.3}$  solar masses (like the LMC) and the metallicity, 1/6 solar. LSBs seem (small statistics) to be in larger galaxies.

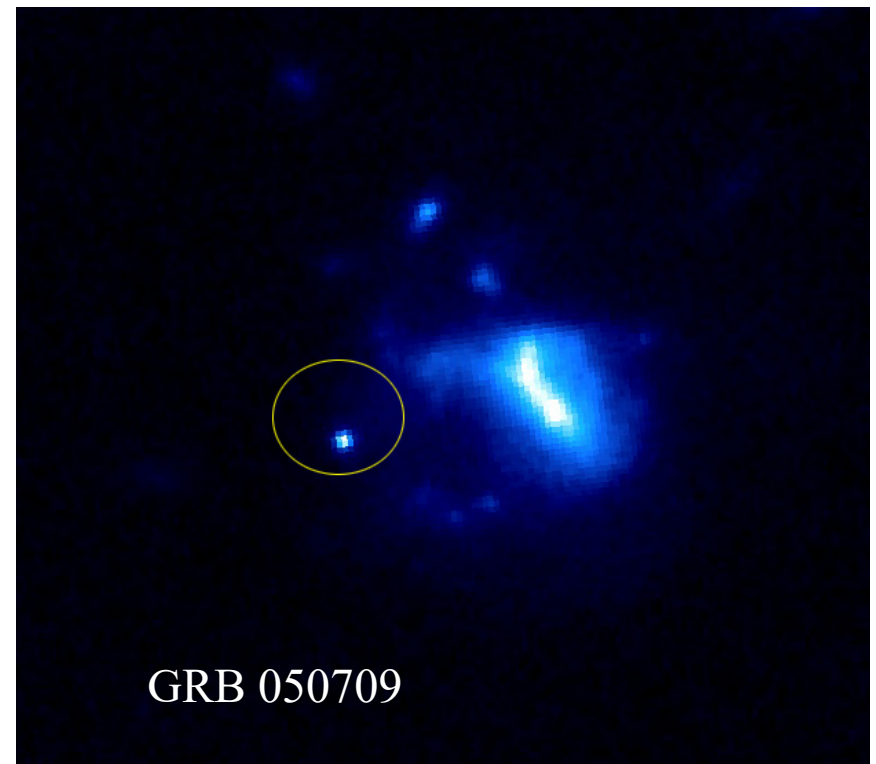
## Additional Predictions Collapsar Model

- Have a time scale governed by the dynamics of the star and accretion, i.e., not a pulsar spin down time
- Separate mechanism for SN and GRB
- At higher redshift (lower metallicity) LSBs should, in general have more total energy and last longer
- Total explosion energies can considerably exceed  $2 \times 10^{52}$  erg (difficult in magnetar model)
- Substantial late time activity due to fallback (Type II collapsar)
- Very long bursts possible from accretion of blue or red supergiant envelope.

# **Short Hard Bursts**



near an elliptical



outskirts of an Ir galaxy

Spectrum of 050724 host galaxy shows it to be an elliptical. SHBs not from massive star death

LS GRBs have much greater energy and brighter afterglows.

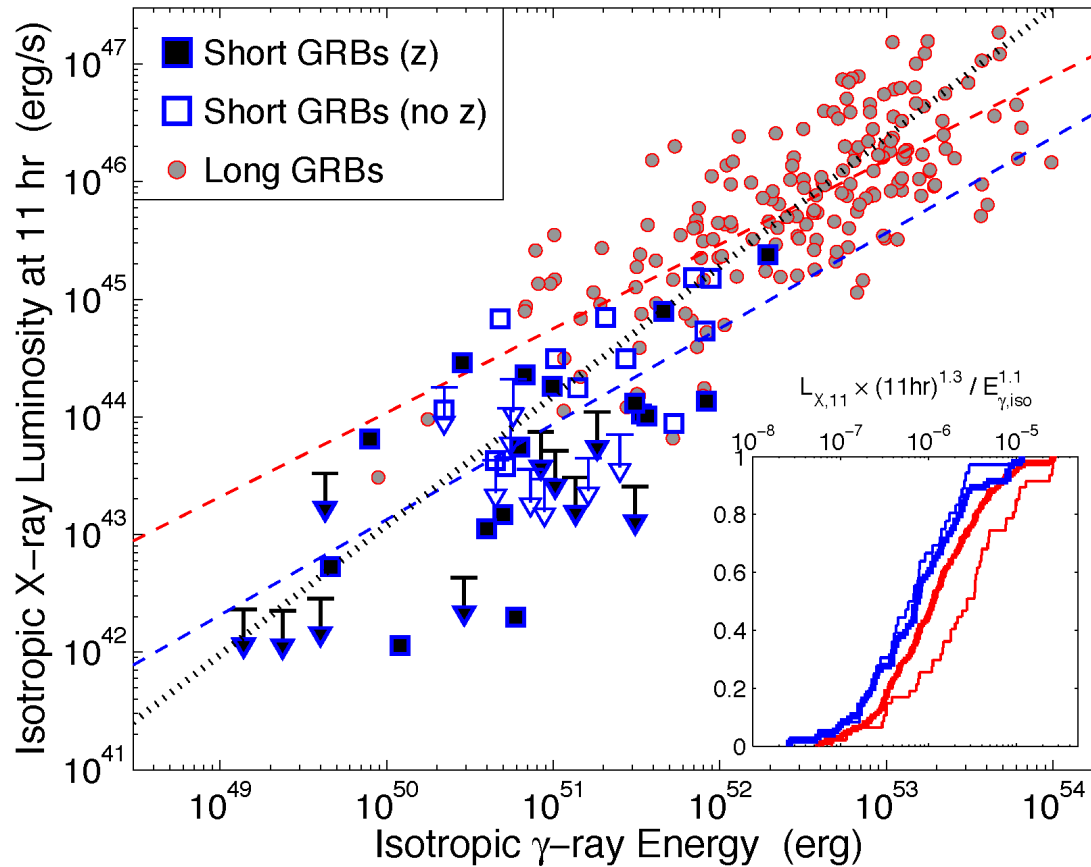
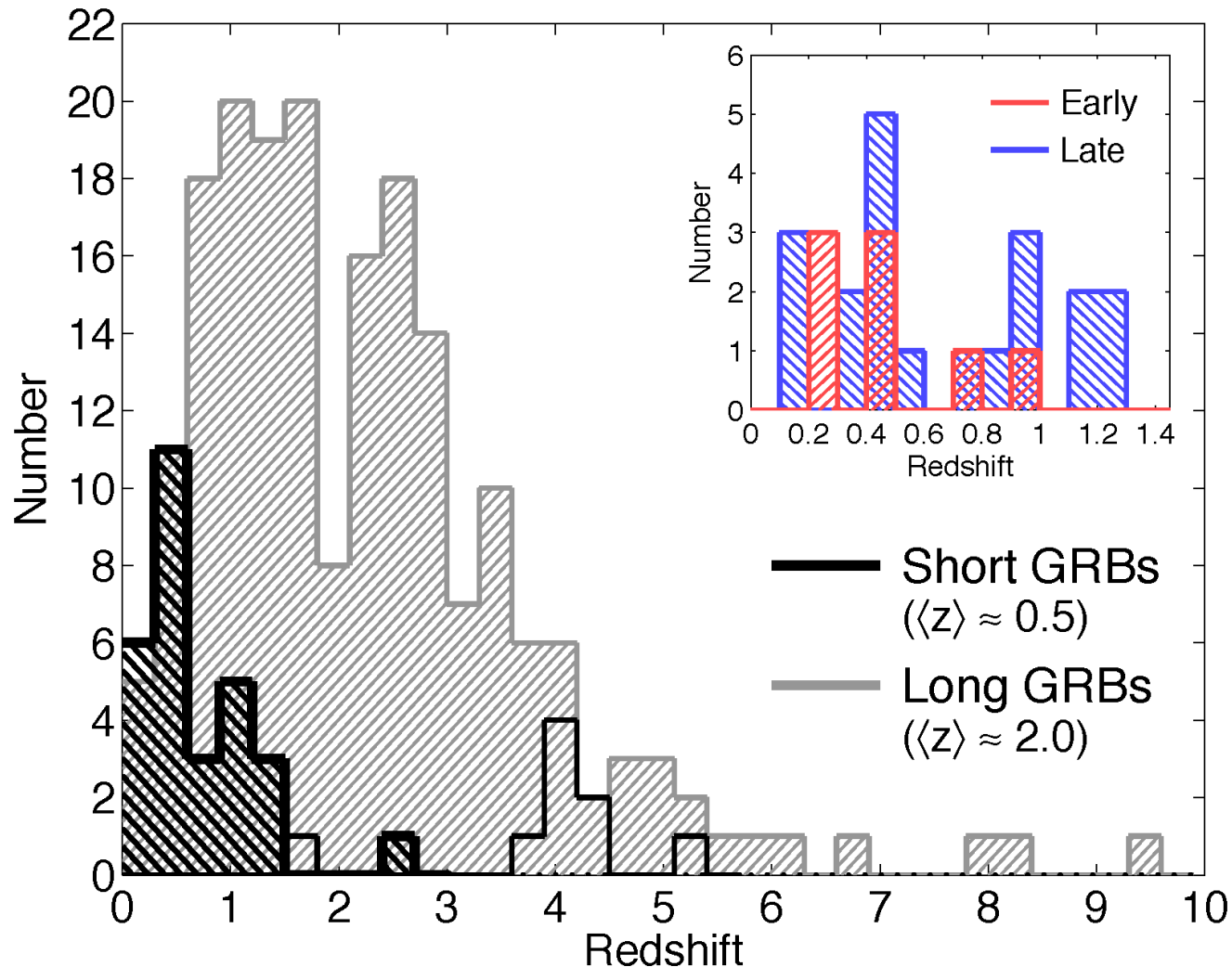


**Figure 14:**

Isotropic-equivalent afterglow X-ray luminosity at a rest-frame time of 11 hr ( $L_{X,11}$ ) versus the isotropic-equivalent  $\gamma$ -ray energy ( $E_{\gamma, \text{iso}}$ ) for short GRBs (blue) and long GRBs (gray). Open symbols for short GRBs indicate events without a known redshift, for which a fiducial value of  $z = 0.75$  is assumed. The dashed blue and red lines are the best-fit power law relations to the trends for short and long GRBs, respectively, while the dotted black line is the expected correlation based on the afterglow synchrotron model with  $\nu_X > \nu_c$  and  $p = 2.4$  ( $L_{X,11} \propto E_{\gamma, \text{iso}}^{1.1}$ ). The inset shows the distribution of the ratio  $L_{X,11} \times (11 \text{ hr})^{1.3} / E_{\gamma, \text{iso}}^{1.1}$ , for the full samples (thick lines) and for bursts in the region of  $E_{\gamma, \text{iso}}$  overlap (thin lines). The lower level of  $L_{X,11}$  relative to  $E_{\gamma, \text{iso}}$  for short GRBs is evident from these various comparisons.

SH GRBs are sampled in a much smaller volume presumably because they are fainter and briefer and thus harder to detect.



Berger (2013)

**Figure 4:**

The redshift distribution of short GRBs (black) and long GRBs (gray). The open histogram marks redshift upper limits based on the lack of a Lyman- $\alpha$  break in afterglow and/or host galaxy optical detections. The inset shows the redshift distribution of short GRBs separated by host galaxy type, which exhibits no discernible difference between early-type (red) and late-type (blue) hosts.

## some association with star formation

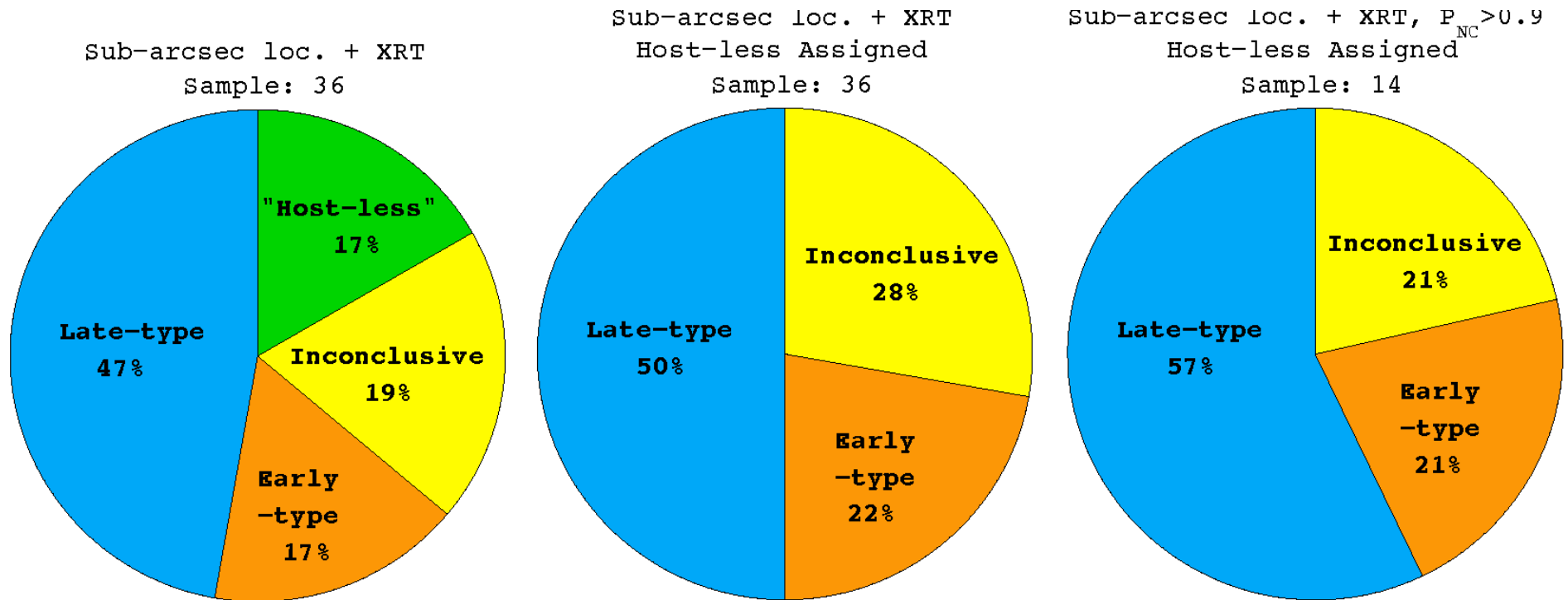


**Figure 5:**

Demographics of the galaxies hosting short GRBs. *Left:* A breakdown into late-type (blue), early-type (orange), host-less (green), and inconclusive (yellow) for all identified hosts based on sub-arcsecond positions and *Swift*/XRT positions (Table 2). *Middle:* Same as the left panel, but with the host-less events assigned to the other categories based on the galaxies with the lowest probability of chance coincidence in each case (Berger 2010, Fong & Berger 2013). *Right:* Same as the middle panel, but for short GRBs with a probability of a non-collapsar origin of  $P_{\text{NC}} \gtrsim 0.9$  based on the analysis of Bromberg et al. (2013). Regardless of the sample selection, late-type galaxies dominate the host sample. This indicates that star formation activity plays a role in the short GRB rate. Adapted from Fong et al. (2013).

SH GRBs show a preference for larger galaxies (i.e., more mass means more of everything). LS GRBs prefer smaller (lower metallicity) star forming galaxies.

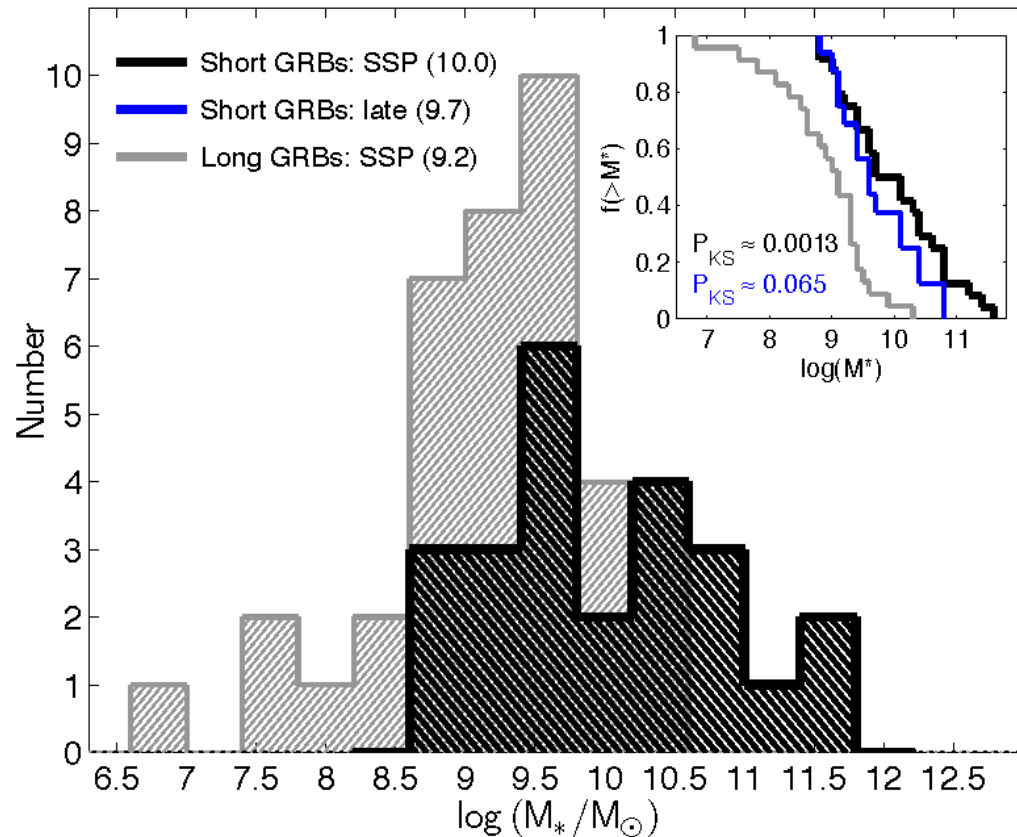
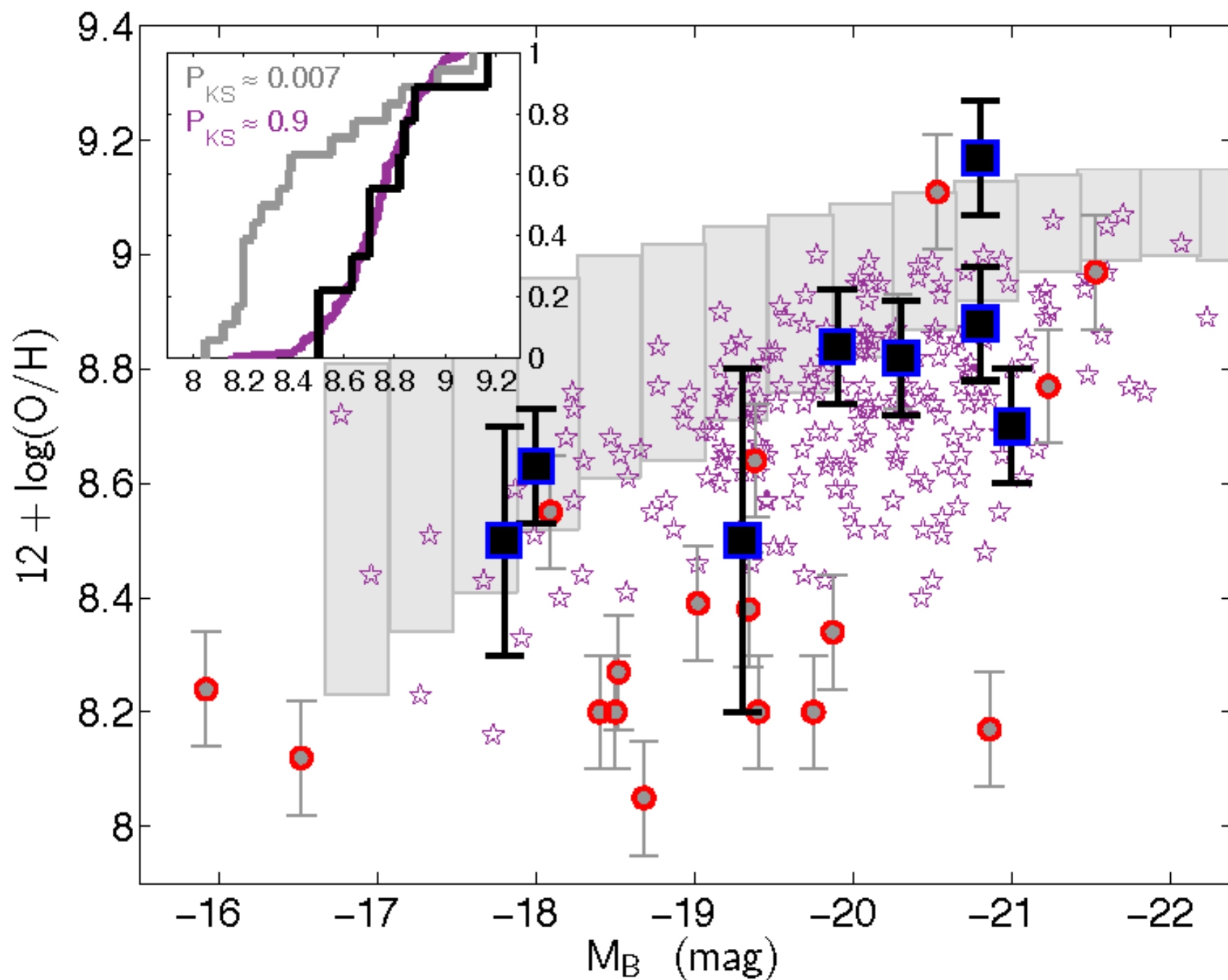


**Figure 6:**

*Left:* Histogram of host galaxy stellar masses for s



Metallicity of hosts: Circles are LS GRBs, squares are SH GRBs. Stars and bands are normal galaxies. Long bursts prefer preferentially at low metallicity. Short bursts do not.

SH GRBs are offset from the main light of their host galaxies by much more than LS GRBs. Their distribution is consistent with that expected for merging neutron stars

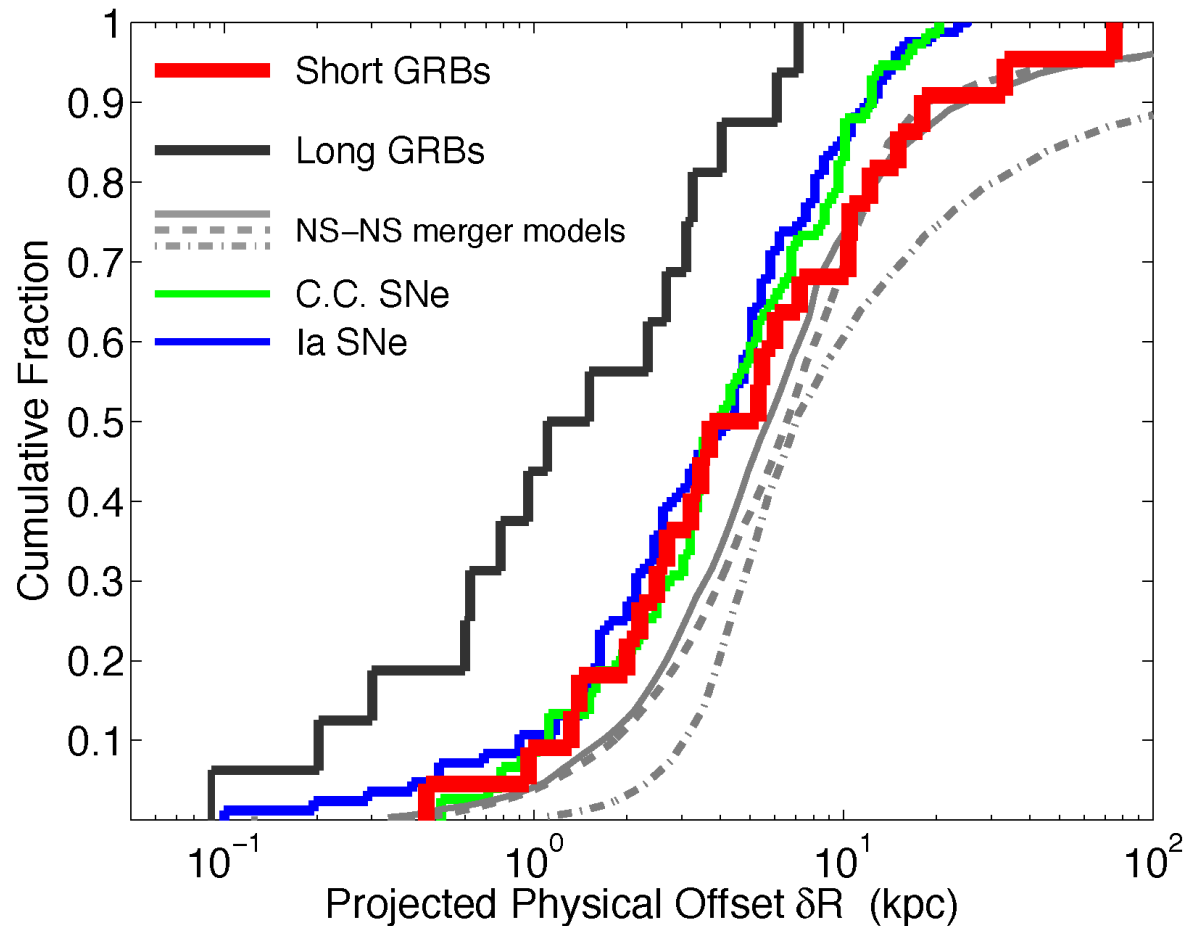
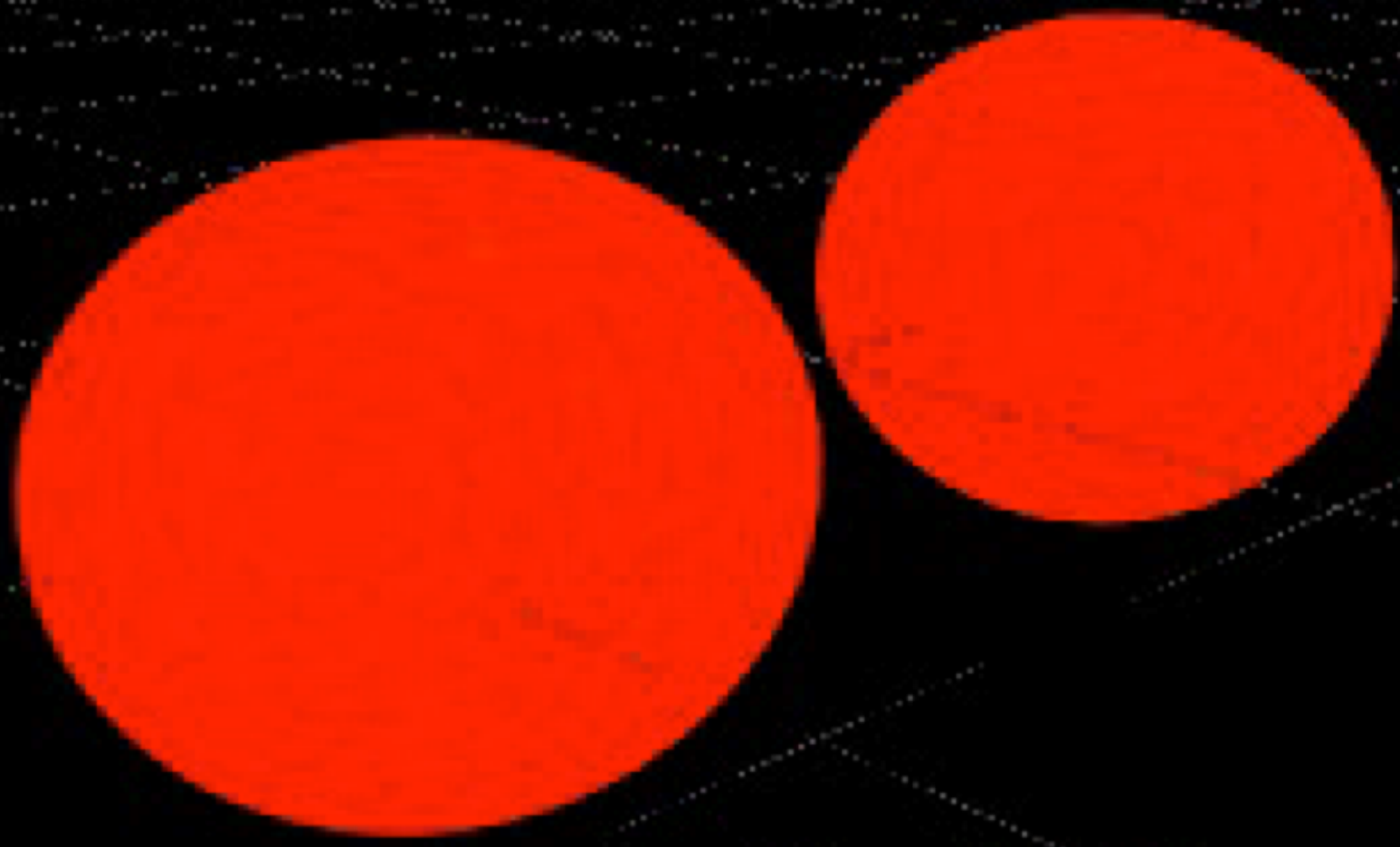


**Figure 10:**

Cumulative distribution of projected physical offsets for short GRBs with sub-arcsecond positions (red; Fong, Berger & Fox 2010; Fong & Berger 2013), compared to the distributions for long GRBs (black; Bloom, Kulkarni & Djorgovski 2002), core-collapse SNe (green; Prieto, Stanek & Beacom 2008), Type Ia SNe (blue; Prieto, Stanek & Beacom 2008), and predicted offsets for NS-NS binaries from population synthesis models (grey; Bloom, Sigurdsson & Pols 1999; Fryer, Woosley & Hartmann 1999; Belczynski et al. 2006). Short GRBs have substantially larger offsets than long GRBs, and match the predictions for compact object binary mergers. From Fong & Berger (2013).



Rosswog (2003)

FERMI detected a short GRB accompanying GW 170817 starting 2 s after the GW detection. GRB170817A. We know this involved a neutron star merger

Fluence  $2.8 \times 10^{-7}$  erg cm<sup>-2</sup> duration 2 s distance 40 Mpc implies an isotropic equivalent energy of  $5 \times 10^{46}$  erg. This is three to four orders of magnitude less than the typical short GRB. Further the pulse had an unusual spectrum consisting of two parts – soft and hard.

Kasliwal et al (2017) argue that the burst was produced by a jet with Lorentz factor  $> 2.5$ , much faster than the bulk of the ejecta ( $\Gamma < 1$ ) that made the r-process and the kilonova

(Gottlieb et al 2018, MNRAS)

shock breakout from the envelope of the star. In the latter the shock breakout is from the surrounding matter (ejecta) that is thrown out to space during the merger process.

Mooley et al (Nature 2018) say “the radio data require the existence of a mildly relativistic wide-angle outflow moving towards us.” It is not consistent with a jet viewed off axis.

Gottlieb et al 2018

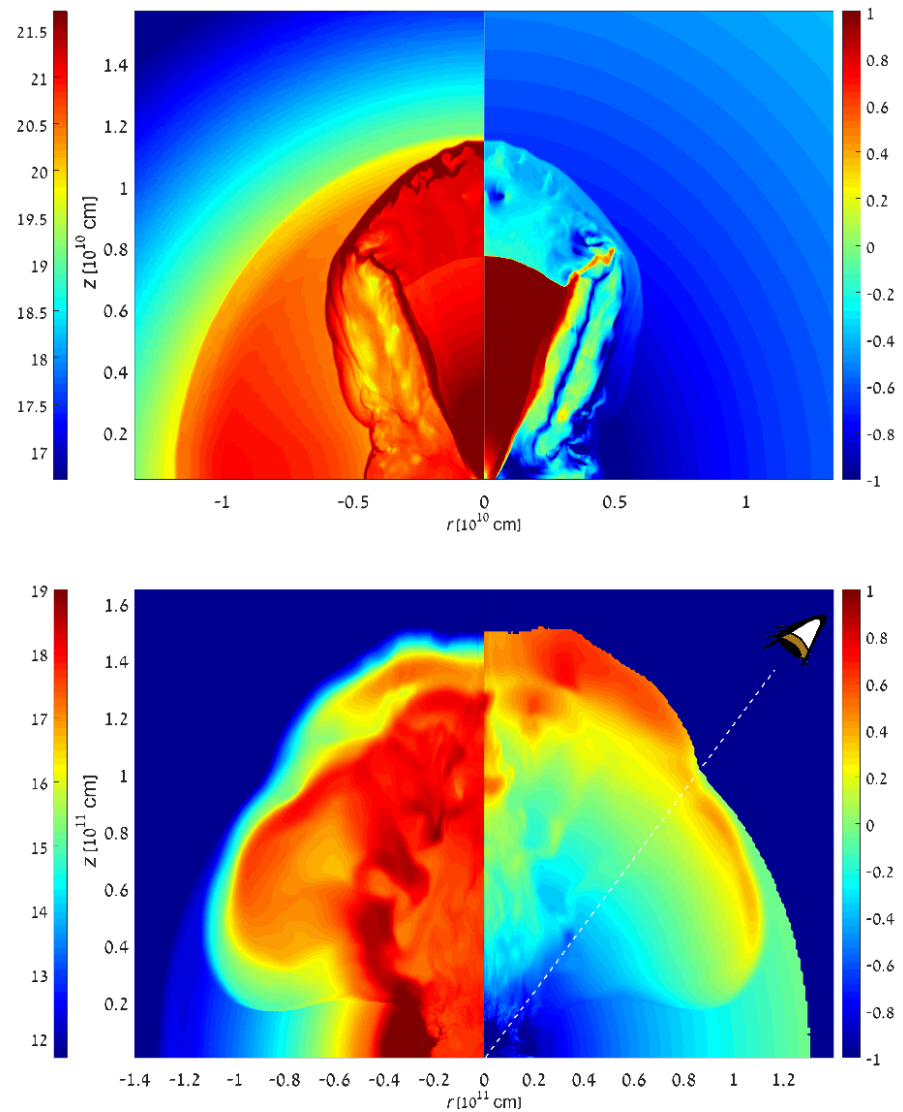


**Figure 1.** Maps of the logarithmic energy density excluding the rest-mass energy (left) in c.g.s units and logarithmic four velocity (right). The upper figure is taken before the breakout of the forward shock from the core ejecta. Although the forward shock will breakout, the jet material behind the reverse shock will remain trapped inside and will be choked with the termination of the engine. The lower figure is taken when the shock breaks out of the tail at  $\theta = 0.7\text{rad}$  at  $t = 6.2\text{s}$  and  $r = 1.3 \times 10^{11}\text{ cm}$ . The shock has a quasi-spherical shape, reaching most of the ejecta. (An animation is available in the online journal.)

kilonova papers from ucsc:

Kirkpatrick et al - Electromagnetic evidence that SSS17a is the result of a neutron star merger

<http://science.sciencemag.org/content/sci/358/6370/1583.full.pdf>

Siebert et al – The unprecedented properties of the first electromagnetic counterpart to a gravitational wave source

<https://iopscience.iop.org/article/10.3847/2041-8213/aa905e/pdf>

Others

<https://reports.news.ucsc.edu/neutron-star-merger/research/>

# SCIENTIFIC PAPERS FROM THE 1M2H COLLABORATION

-  Coulter et al., *Science*, "[Swope Supernova Survey 2017a \(SSS17a\), the Optical Counterpart to a Gravitational Wave Source](#)"
-  Drout et al., *Science*, "[Light Curves of the Neutron Star Merger GW170817/SSS17a: Implications for R-Process Nucleosynthesis](#)"
-  Shappee et al., *Science*, "[Early Spectra of the Gravitational Wave Source GW170817: Evolution of a Neutron Star Merger](#)"
-  Kilpatrick et al., *Science*, "[Electromagnetic Evidence that SSS17a is the Result of a Binary Neutron Star Merger](#)"
-  Siebert et al., *ApJL*, "[The Unprecedented Properties of the First Electromagnetic Counterpart to a Gravitational-wave Source](#)"
-  Pan et al., *ApJL*, "[The Old Host-galaxy Environment of SSS17a, the First Electromagnetic Counterpart to a Gravitational-wave Source](#)"
-  Murguia-Berthier et al., *ApJL*, "[A Neutron Star Binary Merger Model for GW170817/GRB170817a/SSS17a](#)"
-  Kasen et al., *Nature*, "[Origin of the heavy elements in binary neutron star mergers from a gravitational wave event](#)"
-  Abbott et al., *Nature*, "[A gravitational-wave standard siren measurement of the Hubble constant](#)" (The LIGO Scientific Collaboration and The Virgo Collaboration, The 1M2H Collaboration, The Dark Energy Camera GW-EM Collaboration and the DES Collaboration, The DLT40 Collaboration, The Las Cumbres Observatory Collaboration, The VINROUGE Collaboration & The MASTER Collaboration)
-  Abbott et al., *ApJL*, "[Multi-messenger Observations of a Binary Neutron Star Merger](#)"